CHARACTERISATION OF MECHANICAL, THERMAL, FLAMMABILITY AND WATER ABSORPTION PROPERTIES OF BAMBOO FABRIC REINFORCED POLYMER COMPOSITE MATERIALS

Thesis

Submitted in partial fulfilment of requirements for the degree of

DOCTOR OF PHILOSOPHY

by

GANGADHAR M KANAGINAHAL
Reg. No. 177008ME003

DEPARTMENT OF MECHANICAL ENGINEERING
NATIONAL INSTITUTE OF TECHNOLOGY KARNATAKA
SURATHKAL, MANGALORE – 575025

March, 2022

CHARACTERISATION OF MECHANICAL, THERMAL, FLAMMABILITY AND WATER ABSORPTION PROPERTIES OF BAMBOO FABRIC REINFORCED POLYMER COMPOSITE MATERIALS

THESIS

Submitted in partial fulfilment of requirements for the degree of
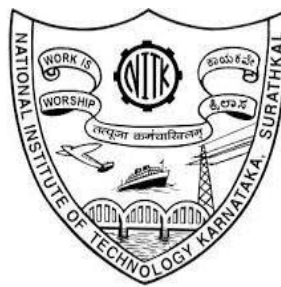
DOCTOR OF PHILOSOPHY

by

GANGADHAR M KANAGINAHAL
Reg. No. 177008ME003

Under the guidance of

Dr. H. Suresh Hebbar
Professor

DEPARTMENT OF MECHANICAL ENGINEERING
NATIONAL INSTITUTE OF TECHNOLOGY
KARNATAKA
SURATHKAL, MANGALORE – 575025

March, 2022

DECLARATION

I hereby declare that the Research Thesis titled **"CHARACTERISATION OF MECHANICAL, THERMAL, FLAMMABILITY AND WATER ABSORPTION PROPERTIES OF BAMBOO FABRIC REINFORCED POLYMER COMPOSITE MATERIALS"** which is being submitted to the **National Institute of Technology Karnataka, Surathkal** in partial fulfillment of the requirements for the award of the degree of **Doctor of Philosophy** in **Department of Mechanical Engineering** is a *bonafide report of the research work carried out by me*. The material contained in this Research Thesis has not been submitted to any other Universities or Institutes for the award of any degree.

Register Number: 177008ME003

Name of the Research Scholar: **Gangadhar M Kanaginahal**

Signature of the Research Scholar:

Department of Mechanical Engineering

Place: NITK-Surathkal

Date: 30|03|2022

CERTIFICATE

This is to certify that the Research Thesis titled **"CHARACTERISATION OF MECHANICAL, THERMAL, FLAMMABILITY AND WATER ABSORPTION PROPERTIES OF BAMBOO FABRIC REINFORCED POLYMER COMPOSITE MATERIALS"** submitted by **Mr. Gangadhar M Kanaginahal (Register Number: 177008ME003)** as the record of the research work carried out by him, *is accepted as the Research Thesis submission* in partial fulfillment of the requirements for the award of the degree of **Doctor of Philosophy.**

30/03/2022

Dr. H. Suresh Hebbar
Research Guide

Chairman-DRPC

Date: 30.3.2022

ACKNOWLEDGEMENTS

I would like to take this opportunity to express my gratitude to my father **Mr. Mallappa B Kanaginahal** and mother **Mrs. Renuka M Kanaginahal** who believed in me, stood by me all the time and have kept encouraging me in difficult times. I am truly blessed to have my wife **Smt. Rajeshwari S Sankangoudar** for being there with me all time, for her love and affection towards me. I thank my younger brother **Mr. Santosh M Kanaginahal**, my younger sister **Mrs. Sangeetha V Talugeri** and my brother-in-law **Mr. Vinayak V Talugeri** for their support, encouragement and love towards me all the time.

I would like to express my sincere thanks towards **Dr. S. Srinivas**, Professor, Department of Mechanical Engineering, **Dr. M. Ramachandra**, Professor, Department of Mechanical Engineering, **Dr. B N Sarada**, Professor, Department of Mechanical Engineering and **Mr. Madhav Murthy**, Assistant Professor, Department of Mechanical Engineering, BMS College of Engineering, Bengaluru for being there during difficult times, supporting me, encouraging me and providing facilities for completion of my research work. I would like to express my gratitude to **Dr. Siddaramaiah**, Professor and Head, Department of Polymer Science and Technology, Sri Jayachamarajendra College of Engineering, Mysore for providing facilities to conduct testing of samples.

Finally I want to express my gratitude to **Mr. Mohan Kumar**, **Mr. Vijay Rampure**, **Mr. Raviteja S**, **Mr. Yashas Sudarshan**, **Mr. Abhilash Rajendra**, **Dr. Vishwas Mahesh, Mr. Vinayak Kallanavar**, **Mr. Chetan H C**, **Mr. Sohail Bakshi**, **Mr. Ashiq Bellary**, **Mr. Rakesh Patil**, **Mr. Nagesh M**, **Mr. Sachin Hirranaiah**, **Mr. Arun D S**, **Mr. Vishwanath Bajantri, Mr. Satish K** and **Dr. Kiran Shapurkar** who have been there for me during difficult times, supported me, encouraged me and helped me all times..

Gangadhar M Kanaginahal.

National Institute of Technology Karnataka, Surathkal

Date:

Abstract

Natural Fiber Reinforced Polymer Composites have been used immensely in low load bearing applications such as leaf springs, bumpers and boat hulls. Natural fibers are known for their bio-degradability, specific strength and stiffness and ease of extraction. In present work, Plain weave and Twill weave bamboo fabric of 125 gsm were used as reinforcements with medium viscous epoxy B-11 resin and AI 1041 bio-based hardener. Fiber weight fraction was maintained at 18% and composite plates of thickness 3.1, 4.3 and 5.4 mm of plain and twill weave composite were used for study. The aim was to study the influence of weave pattern and thickness of composite on the tensile, flexural, izod impact, thermal, dynamic, water absorption and flammability studies. Fourier Transform Infra-Red results showed the presence of cellulose, polysaccharides in fabric, cardanol groups in resin and hydrogen bonding of reinforcement and matrix. X-Ray Diffraction peaks displayed higher intensities for twill weave fabric indicated high amount of cellulose available for bonding. Tensile studies of fabrics showed 7% higher strength for twill weave compared to that of plain weave fabric in warp direction. Twill weave composites with 5.4 mm thickness showed an increase of 12% in tensile strength and 8% increase in stiffness compared to plain weave. Twill weave composite with 5.4 mm thickness showed an increase of 22% in flexural strength and 28% in stiffness compared to plain weave. Izod impact results displayed an increase of 16% in absorbed energy for 5.4 mm thickness twill weave composite when compared with plain weave. Fractography of tensile tested specimens displayed fiber pullouts for plain weave composites and fiber breakage for twill weave composites. Twill weave composites have shown better wettability than that of plain weave. Weave pattern and composite thickness had negligible influence on thermal degradation of composites Thermo-gravimetric analysis showed a higher thermal stability for composites sustainable till 450 ⁰C, compared to their fabrics. Differential Scanning Calorimetry studies displayed melting of composites at 370 ⁰C. Dynamic mechanical analysis indicated an improvement of 1.3 times in storage modulus for 5.4 mm thickness twill weave compared to plain weave composite. Loss modulus showed a 9% improvement for 5.4 mm thickness twill weave compared to plain weave composite. Loss factor showed

better damping properties for 5.4 mm thickness twill weave compared to plain weave composite. Cole-Cole plot indicated a homogenous interface for 5.4 mm thickness twill weave compared to plain weave composite. Twill weave were effective in hindering water absorption compared to plain weave composites and it was higher at 5.4 mm thickness. Wettability and thickness of composites hindered the burning rate and a 30% reduction was observed at 5.4 mm thickness.

Table of Contents

List of Figures

List of Tables

CHAPTER I

INTRODUCTION

Bricks reinforced with straws were one of the early composites used by Egyptians to build pyramids. Composites are very well established materials replacing the conventional materials in almost all areas. Processing of natural fibers consumes nearly half of the energy compared to synthetic fibers thus grabbing the attention to be chosen as replacement for synthetic fibers in composites. Natural fibers have addressed issues such as recycling, pollution, availability of petroleum products and cost. Natural fiber composites (NFC) have few advantages such as minimized tool wear during machining, fewer health problems, availability, bio-degradability and economical when compared with synthetic fibers. NFC have found applications in roof tops, casing for gears, doors, window frames, flooring, acoustic insulation panels and laptop covers.

1.1 Natural Fiber (NF)

NF have been classified based on their extraction from plants, animals and minerals. Few advantages such as lower processing cost, low density and high specific strength and stiffness have made them acceptable for domestic applications. Few drawbacks such as moisture absorption, durability of performance and operating temperatures have limited their applications in high performances. Suitable surface treatment of fibers, fiber coatings, use of coupling agents and fiber compatibility with matrix have reduced these drawbacks and improved the functionality.

1.2 Plant/Ligno-cellulosic Fiber

Plant fibers consist of cellulose, hemicellulose, lignin, pectin and wax in primary and secondary cell wall. Microfibrils present in these walls will be oriented at an angle to fiber axis, smaller angles show better strength and stiffness and larger ones ductility. Pectin holds these fibers to stem and wax, acting as a coating protecting these fibers from moisture

absorption. Properties of NF vary according to fibers cultivation, chemical content, presence of defects and extraction methods.

```
                              ┌─────────────────┐
                              │  Natural Fiber  │
                              └────────┬────────┘
        ┌──────────────────────────────┼──────────────────────────────┐
┌──────────────────┐        ┌──────────────────┐        ┌──────────────────┐
│ Lignocellulosic  │        │   Animal Fiber   │        │  Mineral Fiber   │
│     Fiber        │        └──────────────────┘        └──────────────────┘
└──────────────────┘
```

Lignocellulosic Fiber	Animal Fiber	Mineral Fiber
Wood Fiber — **Non-Wood Fiber**	- Silk - Animal hair - Wool - Feathers - Alpaca hair	- Amosite - Crocidolite - Tremolite - Actinolite - Chrysolite
Wood Fiber: - Hardwood - Softwood		

Seed Fibers	Leaf Fibers	Bast Fibers	Fruit Fibers	Stalk Fibers
- Cotton - Kapok	- Sisal - Pineapple - Abaca - Henequen	- Flax - Banana - Hemp - Jute - Kenaf	- Coir - Oil Palm	- Rice - Barely - Wheat - Maize - Bamboo

Figure 1.1: Classification of Natural Fibers
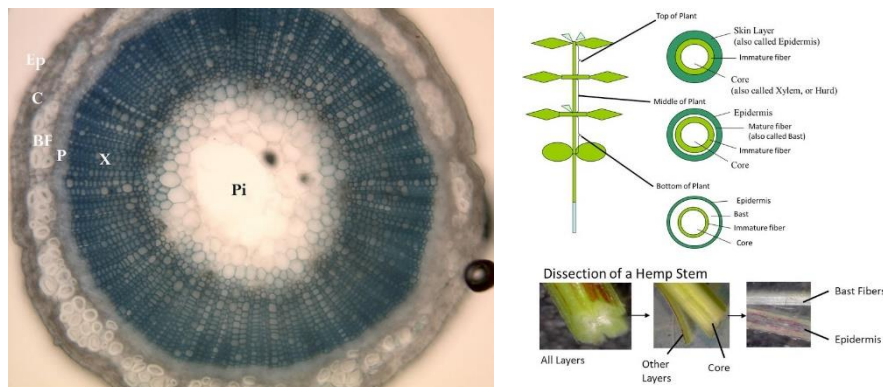
Figure 1.2: Section of stem [Courtesy: Wikipedia]
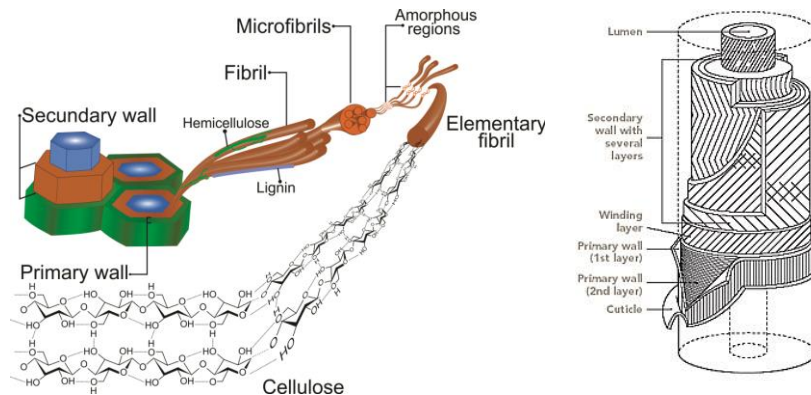
Figure 1. 3: Basic structure of natural fiber [Courtesy: Wikipedia]

1.3 Stalk Fibers

Bamboo

Azeez and Orege (2013) have stated that stems of bamboo have been utilized in making of cellulose, starch and bio-ethanol. Tensile strength of bamboo has been considered in par with that of mild steel. Few studies done on bamboo fibers subjected to alkali treatment have shown better dielectric properties, tensile and flexural strength. Mercerised bamboo treated with silane have shown reduction in strength. Bamboo has been used in applications such as pipes for supply of water, passage for drainage, as a reinforcement for concrete, floor tiles, cupboards, mats and composites. Osorio et al. (2018) stated that the mechanical properties of bamboo were defined by secondary wall elementary fibrils tapered at both ends surrounding a hollow space known as lumen. Zakikhani et.al. (2014) stated that bamboo fibers have 73.83% cellulose and 10.15% lignin. The elementary fibrils were glued by lignin and hemicellulose, forming vascular bundles around the culm.

Figure 1. 4: Bamboo Fiber [Courtesy: Kiron (2011), guaduabamboo.com]
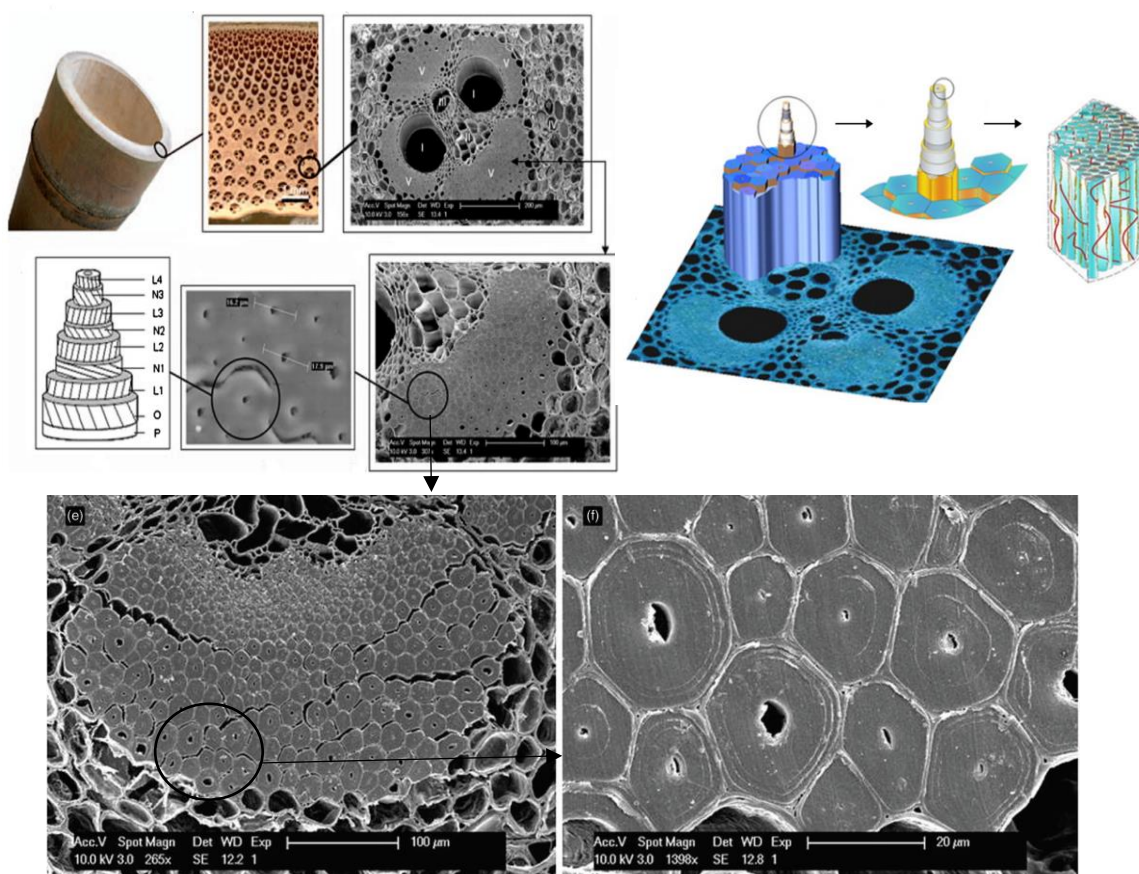
Figure 1. 5: Bamboo Structure, Fiber bundle and Elementary fiber with lumen [Courtesy: Zakikhani et.al. (2014), Osorio et al. (2018)]

The fibers have been extracted by processes such as mechanical, chemical and combination of both. Mechanical processes such as in a) Steam explosion – the strips cut from bamboo were subjected to steam where fibrils got detached from each other through removal of

lignin, b) Retting - the strips were kept in water for several days and later beaten to hard substance and the surface was peeled by a knife, c) Crushing - small bamboo pieces cut from plant were crushed by roller to extract coarse fibers, d) Grinding - small strips were grinded at a speed and the fibers were separated by passing them through sieves, e) Rolling - strips soaked in water were passed through rolling mills and soaked again, later the fibers were separated by blades and sun dried. Chemical processes such as a) Degumming – gummy portion and pectin were removed to separate the fibers, b) Alkali retting – by soaking in sodium hydroxide (NaOH) solution unwanted materials were removed such as lignin, hemicellulose, c) Chemical retting – by treating with various chemicals such as sulphuric acid, sodium silicate etc. unwanted materials were removed to separate fibers.

Properties

- Better drape-ability and breathability
- Resistant to microbes, quick drying, acts as thermal regulator and anti-Ultraviolet (UV)
- Soft, silky and easy to weave into fabric.

Applications

Bandages, swimwear, fabrics, masks and curtains.

1.4 Woven Fabrics

Warp and weft are two directions considered in weaving pattern which are oriented at 90° to each other. For bi-directional woven fabrics most of materials were woven of same material, also different materials have been used to achieve hybrid.
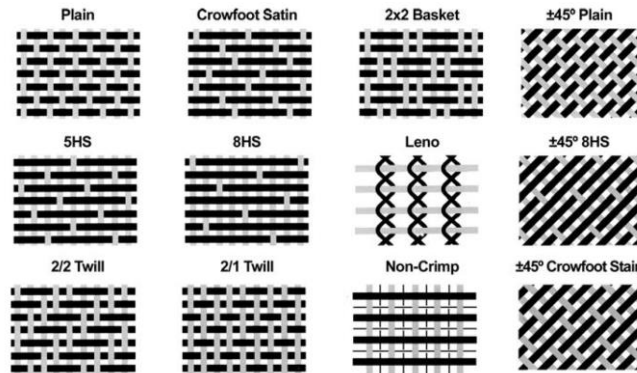
Figure 1. 6: Different types of weave patterns [Courtesy: Mazumdar (1977)]

Plain weave is a basic form of weave pattern used widely across industries and other applications. Its strength deteriorates due to the waviness formed during weaving from top to bottom. It has been apt for flat materials only. Basket weave with two up and two down weave pattern may not be symmetrical and the weaving counts may vary. With less waviness than plain weave it has been used for contour parts production. Twill weave has displayed better wettability and strength than plain weave pattern. Satin weave is a form where if x yarns are in warp then x-1 yarns will be in fill, example (e.g.) in 5HS - 5 harness, 5 yarns used in warp and 4 yarns in fill direction.

1.5 Fiber-Surface Treatment

NF composed of cellulose, lignin, pectin and so on, cellulose are made of hydroxyl groups (-OH) that defines their hydrophilicity. NF have crystalline and amorphous cellulose structure, of which amorphous region have displayed greater affinity towards water absorption. Pectin acts as a biological glue holding the fibrils from primary cell wall to the secondary. Treatments were necessary to remove some of unwanted materials such as lignin, pectin, waxes which hinder the properties of NF. Removal of pectin eases removal of other non-cellulosic materials. The physical, chemical and mechanical treatments have been mentioned as below –

Physical - At low temperatures the plasma treatment changes the surface by etching and crystallization. During plasma treatment fiber surface functional groups were converted by unstable radicals and may vary the surface roughness.

Chemical – Mercerization, an alkaline treatment where the hydroxyl groups were substituted by sodium ions act as water resistant making NF hydrophobic.

Coupling agents – Silanes and titanate based compounds which act as bonding agents between fiber hydroxyl groups and matrix functional groups improve the adhesion.

1.6 Thermoset polymers

Curing of thermoset forms a cross-linking structure with strong covalent bonds making them insoluble and infusible, such that only at high temperatures they regain their shape. They can be cured at low temperatures and are economical too. Polyesters, epoxy, vinyl ester, phenolics, cynate ester and so on are few types of thermosets

1.6.1   Epoxy

Economical cost, resistance to environmental degradation, better performance and resistant to water degradation have made them suitable for aircraft industries. A curing agent known as a hardener will be always added with epoxy, which defines the performance of epoxies. Addition of hardeners also have an influence on enhancing the Glass Transition Temperature (T_g) of epoxies. Epoxies cure slowly thus application of heat will enhance the curing rate. Epoxies have a molecular structure with epoxy groups as side reactive sites which undergo reaction with hardeners forming a three dimensional network

1.7 Hardeners

Amines and anhydrides are typically used for epoxies which have high toxicity and require heating to cure. Latent hardeners are unreactive at low temperatures but will form bonding at high temperatures such that the final component has better properties. Amine hardeners cure at low temperatures but undergo exothermic reactions, whereas anhydries need an

accelerator for curing. Using an amine hardener, the ratio of resin to hardener has to be determined to minimize the inefficiency after cure.

1.7.1 Phenalkamine

Phenalkamines, known for fast curing at very low temperatures, with excellent moisture and chemical resistance have gained importance in marine coatings. They were synthesized from cardanol i.e. extracted from cashew nut shell liquid. The aliphatic side chain of cardanol provides a good pot life and they have excellent resistance to salt water conditions. Their hydrophobic nature ensure surface resin bonding even on wet surfaces.

1.8 Interface

Interface a two dimensional (2-D) boundary formed between surfaces of reinforcement and matrix shows better results for rough fiber surfaces and minimum fiber diameter. A brittle material will have strong interface with better strength and stiffness or it will be ductile with maximum fracture resistance. At interface achieving better bonding may sometimes lead to brittleness of material because of which it must show toughness along with better strength. Agglomeration, wettability, crystal structure and bonding are few parameters which influence interface properties. Few tests such as flexural, short beam shear, single fiber pull-out, iosipescu shear, indent test, laser spallation and fragmentation tests have been conducted to study the interface properties.
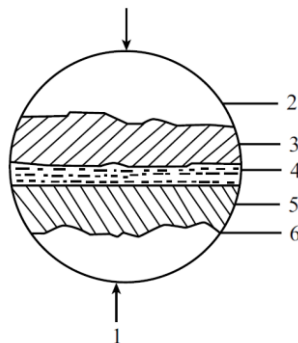
Figure 1. 7: Interface (1. External surface, 2. Bulk matrix, 3. Matrix surface zone, 4. Mutual infiltration zone, 5. Fiber surface zone, 6. Bulk fiber) [Courtesy: Wang. R. M. et.al. (2011)]

CHAPTER 2

LITERATURE REVIEW

2.1 Short Fibers reinforced composites

Dong et al. (2014) treated 6 mm to 8 mm length coir fibers of 0.15 mm to 0.25 mm diameter in NaOH solution and piled them between Poly lactic acid (PLA) sheets. Tensile Modulus (TM) determined was highest at 5 Weight Percentage (wt%) and Flexural Modulus (FM) was highest at 20 wt% for untreated coir/PLA. Tensile Strength (TS) and Flexural Strength (FS) observed were lower than neat PLA because of voids, cracks on fiber surface and agglomeration of fiber. Unwetted fibers at higher fiber percentage showed an increase in elongation. Fiber treatment hastened the fiber degradation compared to untreated fiber.

Dayo et al. (2017) worked on 5 mm length hemp fibers treated with ethanol/cyclohexane and NaOH and processed them into laminates by Polybenzoxazine (PBA). Fourier Transform Infrared Spectroscopy (FTIR) graphs notified peaks at 1000 cm^{-1} for hydroxyl groups, at 1420-1520 cm^{-1} were due to the removal of lignin, at 1650 cm^{-1} was because of removal of partial hemicellulose and at 3420 cm^{-1} due to hydrogen bonding for cured samples. Differential Scanning Calorimeter (DSC) curves indicated enhancement of treated Fiber Volume fraction (V_f) reduces the curing time. Higher storage modulus, lower damping and an increase in Glass transition temperature (T_g) results obtained from Dynamic Mechanical Analysis (DMA) indicated better load transfer with an increase in treated V_f. FS, FM, TS and impact values at 25 wt% treated fibers/PBA were higher compared to neat PBA. Differential thermal gravimetric (DTG)/ Thermal gravimetric analysis (TGA) results indicated loss of moisture at 105 °C. 21.1% char was observed for raw and 19.7% for treated fibers which notified loss of material reduced by treatment. Water absorption showed a linear intake with an increase in fiber percentage.

Sullins et.al. (2017) analysed hemp fibers treated with 5 wt% and 10 wt% NaOH and stacked them into laminates by Polypropylene (PP)/Maleic-anhydride grafted polypropylene (MAPP). Peaks noticed at 3200-3500 cm^{-1} and 1104 cm^{-1} from FTIR graphs

were for stretching of hydroxyl groups and C-O-C of cellulose, respectively. FS and FM of composite was highest at 30 wt%-5%NaOH-5%MAPP and TS, TM was highest at 30 wt%-5MAPP. SEM images displayed improper bonding for untreated and treated composites compared to MAPP filled composites.

Costa Júnior et al. (2015) analysed 35 mm length bamboo fibers treated in 5% and 10% NaOH and sodium hypochlorite (NaClO) and processed them into laminates by resol+epoxy. SEM displayed presence of wax on raw fibers and exposure of fibrils for treated fibers. FTIR graphs notified removal of pectins and waxes at 1735 cm^{-1} and loss of lignin at 1253 cm^{-1}. XRD patterns displayed peaks at 18.2°C and 26.0°C of 101 and 002 planes respectively, indicating the presence of cellulose, which increases by 48.28% after treatment. TS of treated fibers/epoxy were higher compared to untreated/epoxy. Differential Thermal analysis (DTA)/TGA curves of treated and untreated bamboo showed loss of water at 100 °C, lignin between 200 to 550 °C and degradation of bio-composites between 250 to 300 °C. In 210 days, treated fiber composites degraded rapidly compared to untreated.

Krishna Adhikari and Keerthi Gowda (2017) processed 10 mm chopped banana and jute fibers in ratio of 1:1 and piled them by Polyester (PE) into laminates. TS was highest for 5 mm thick and 15% V_f composite. Impact strength was highest for 25% V_f and 5mm thick composite.

Wanderson Moreira Ribeiro et al. (2017) worked on NaOH treated short bamboo fibers laminated by PBA. XRD patterns showed an improvement in crystallinity after treatment. FTIR curves notified presence of olefinic hydrogen atoms of cardanol in PBA. Tanδ curves plotted from DMA inferred an increase in stiffness for 10% NaOH treated fiber. TGA showed 10% NaOH treated fibers have better resistance compared to neat matrix.

Balaji et.al. (2017) blended cardanol with bagasse fiber and compressed it at 110 °C. Aromatic rings determined from FTIR curves indicated the presence of cardanol. Poor bonding displayed lower values of TS and FS. Impact properties of composites reduced after 5 wt% addition of fiber. Water absorption was minimum for pure matrix.

Barreto et.al. (2011) processed sisal fibers cut in 20 mm length and treated with 5% and 10% NaOH followed by NaClO/Dihydrogen monoxide (H_2O) and were piled by extracted resole + epoxy. XRD patterns of cellulose increased by 69% for treated. FTIR graphs notified peaks at 1730 cm^{-1} and 3372 cm^{-1} due to removal of unwanted materials and an increase in cellulose percentage, respectively. TGA showed improvement in decomposition rate for treated fibers compared to untreated fibers and inferred better diffusion of resin into fiber. DSC curves showed dehydration till 140 °C i.e. endothermic and from 265 °C exothermic, due to depolymerisation and degradation. DMA studies inferred 10% NaOH treatment improves loading properties.

Leandro et al. (2016) worked on milled sponge gourd fibers treated with NaOH and NaClO and piled them into laminate by resol + epoxy. DSC curves indicated that treatment minimizes the loss of material due to dehydration. An increase of 144.12% in TS for 10% NaOH treated fiber was noticed.

Indira, Parameswaranpillai and Thomas (2013) studied banana fibers of varying length processed into laminate by phenol formaldehyde. TS, elongation to break and FS of 30 mm fiber length at 40 wt% were higher for resin transfer molded composite. Low load bearing capabilities were observed for higher fiber percentage. Impact strength was maximum for 30 mm length fiber at 40 wt% composite fabricated by compression molding. SEM displayed maximum fiber pull-out for compression molded composite than resin transfer molded composite.

Sahoo, Mohanty and Nayak (2016) added short sisal fibers of varying fiber wt% into epoxy/epoxidized soyabean oil and processed them into laminate. Addition of sisal increased the impact strength, TS and TM, compared to a neat matrix. TGA displayed a reduction in the char formation of epoxy by addition of soyabean oil and sisal. Tanδ curves indicated a better load transfer with the addition of sisal as the peaks reduced and broadened, with an increase in T_g.

Banga, Singh and Choudhary (2015) varied the wt% of bamboo fibers of 2 mm length and piled them into laminate by epoxy. With the addition of bamboo, TS and FS of composite

decreased. Hardness at 20 wt% bamboo/epoxy and impact strength at 30 wt% was higher. Water absorption increased with the addition of bamboo.

Essabir et.al. (2016) studied about coir fibers treated in 1.6 moles per litre (mol/l) NaOH and processed them into laminate with coir shells and PP. Under SEM, uniform dispersion of fillers was visible at a ratio of 10:10 in PP, with better wettability of fibers. FTIR graphs indicated the presence of cellulose and hemicellulose for untreated fibers at 2832 cm^{-1} and removal of lignin and hemicellulose at 1252 cm^{-1} and 1734 cm^{-1}, after treatment. TGA curves displayed an enhancement in thermal stability for treated fiber hybrid composites. TS of treated fiber composite with fillers and compatibilizers was higher.

Dhakal and Keerthi Gowda (2017) mixed banana fibers with PE and processed them into laminate. TS increased with an increase in V_f and thickness of the composite. FS increased with an increase in fiber length, V_f and thickness of composite. Impact properties enhanced with the thickness of composite and V_f.

Ogunsile and Oladeji (2016) treated banana fibers with acetic acid and hydrogen peroxide in a ratio of 1:1 and then soaked in 10%NaOH and fabricated them into laminate by LDPE. Characterization of banana fiber showed 47.7% cellulose content in FTIR. Treated fiber composites absorbed less water than untreated. TS showed an improvement by 200% at 20% V_f for treated fibers composite.

Suryawanshi, Venkatachalam and Vimalanand (2016) varied V_f of banana fiber and piled them into laminate by PE and Cashew nut shell liquid (CNSL). Finite element method (FEM) analysis indicated lower percentage of CNSL had higher Stress intensity factor (SIF). Regression analysis showed loss in toughness was due to an increase in CNSL percentage.

Dhanalakshmi, Ramadevi and Basavaraju (2015) extracted areca fibers and treated them with 6% NaOH, 0.5% Potassium permanganate (KMnO$_4$)/acetone solution, benzyl chloride solution, 5% acrylic acid solution at 50°C for 1h, separately. FS of acrylic treated fiber/epoxy at 60% W_f was 126.9% higher than untreated/epoxy.

Nam, Ogihara and Kobayashi (2012) treated coir fibers with varying percentage of NaOH. 10-20 mm length short fibers of varying fiber wt% were fabricated into laminate by PLA. Inter-facial shear strength (IFSS) was higher for 5% NaOH treated fiber/PLA. TS was higher at 20 wt% and TM at 40 wt% for treated fibers/PLA. TGA graphs showed an improvement in thermal stability with increasing fiber wt%. SEM displayed presence of gaps on raw fiber surface and clean surface on treated fibers.

Hybrid Composites

Kiew Liew et.al. (2017) worked on LDPE/short fibers of jute and bamboo treated with ethanol and toluene for dewaxing, followed by treating with acetic acid and NaOH. FTIR graphs showed a rise in cellulose content at 1024-1020 cm^{-1} for treated bamboo and jute, hemicellulose at 1735 cm^{-1} and lignin at 1242.4 cm^{-1}. TS and TM increased by 157% and 195%, respectively for 10wt% treated hybrid composite compared to untreated. SEM displayed better bonding for treated Jute bamboo cellulose composite (JBCC). Treated hybrids of JBCC at 10 wt% had low water absorption compared to untreated.

Biswas et.al. (2013) worked on 5-35 mm length jute, bamboo and coir fibers subjected to tensile condition. Young's modulus increased for longer span length fibers due to reduction in slippage. Calculated elongation was less for bamboo due to bigger diameter. ESEM showed less porosity and rough surface for bamboo and high porosity for coir fiber.

Arrakhiz et.al. (2013) reinforced alfa, coir and sugarcane bagasse short fibers, grinded and treated in solution of 8wt% alkali, later piled by PP into laminate. Alfa/PP at 30 wt% showed highest TM, FS and FM compared to neat PP. DMA studies showed an increase in storage modulus and reduction in loss modulus with the addition of fiber.

Sathish et.al. (2017) mixed 30 mm length flax and bamboo with epoxy and compressed the mixture under pressure of 35 kg/cm^2 at 130 °C for 45min. TS, FS, ILSS and impact strength were higher for flax/epoxy. FTIR graphs indicated presence of crystalline structure of cellulose at 1435-1450 cm^{-1} and amorphous at 876 cm^{-1}. SEM displayed better bonding for flax/epoxy and less fiber pull-outs.

Ying, Wang and Lin (2013) heated a mixture of 50 wt% NaOH treated bamboo fibers with PP fibers in an oven at 80 °C for 48 h. DSC curves displayed an increase in melting temperature (T_m) for heat treated PP and bamboo/PP. Treatment led to arrangement of molecular chains which led to improvement of TS of bamboo/PP and reduction of impact properties.

Wang and Ying (2014) processed NaOH treated bamboo fibers with PP and silane coupling agent into laminate. FTIR analysis notified loss of hemicellulose and lignin at 1640 cm^{-1} for treated fibers. Silane coupling agent and treatment of bamboo increased the TS, TM, FS and FM for 40 wt% bamboo/PP. Treatment reduced water absorption property of bamboo/PP. Addition of bamboo improved T_m and crystallinity of bamboo/PP compared to neat PP. SEM showed better adhesion for treated bamboo/PP compared to raw bamboo/PP. DMA results showed addition of bamboo reduces T_g and damping properties compared to neat PP.

2.2 Long/Woven Fibers reinforced composites

Fiore et al. (2016) soaked sisal fibers into solution of 10wt% sodium bicarbonate (NaHCO$_3$) for 24h, 120h and 240h. TS and IFSS was highest for 120h treatment. FS and FM was maximum for 120h treatment. SEM displayed smooth and bundled surface for raw fibers, fibrillation and reduction in diameter for treated fibers and micro-cracks on the surface of excessively treated fibers. FTIR graphs notified removal of hemi-cellulose and stretching of lignin C-O acetyl group, after treatment. TGA/DTG curves showed loss of weight at 40°C and degradation of sisal at 230°C.

Li, Li and Ma (2015) dried uni-directional flax fibers and stacked them into laminate by epoxy. C-scan showed presence of voids at centre of laminate and inside of yarns, they were reduced by increasing the curing pressure. Pressure applied after 30 min of process showed minimum void percentage. Increased pressure improved the inter-laminar shear strength (ILSS) and TS by 9.67% and 19.46%, respectively. SEM displayed delamination along with matrix cracking for low pressure cured composite.

Francucci, Rodríguez and Vázquez (2010) treated jute fabric with PHB and placed them in mold, under vacuum and passed water/glycerine forming a VARTM process. An increase in V_f showed drop in permeability due to absorption of water/glycerine by the fiber and micropores. Saturated permeability increased the flow rate and bulk permeability was directly proportional to the reinforcement saturation. Treated fabrics showed better permeability compared to untreated. Permeability of PHB treated fibers was better due to the reduction in fibrillation and micro-pores.

Milanese, Cioffi and Voorwald (2012) thermal treated woven sisal and piled them into laminate by phenolic resin. The treated/phenolic and untreated fibers/phenolic had similar FS i.e. 28% more than pure phenolic resin. TGA curves showed initial loss of moisture at 150°C, loss of lignin at 260°C and cellulose at 315°C

Tran et.al. (2013) soaked extracted coir fiber in 5% NaOH and piled them into laminate by PP and Polyvinylidene fluoride (PVDF)/MAPP. IFSS was better for PP than PVDF/MAPP. Coir/MAPP performed better than coir/PP due to covalent bonding of fiber and matrix at interface.

Londhe, Mache and Kulkarni (2016) soaked jute fiber mat in 18% NaOH and stacked them into laminate by epoxy. Treated and acrylic painted specimens had better resistance to moisture in distilled and pH solutions. TS of treated fiber at 30 wt% was maximum.

Rahman, Jasani and Ibrahim (2017) arranged banana fibers treated with 5% NaOH in mold and infused it with epoxy under vacuum. FS was higher for banana/epoxy at 40% V_f.

Chandrasekaran et.al. (2017) stated that alkalisation treatment aligned the cellulose in fiber and reduced its performance. Fiber subjected to less concentration of alkaline and shorter periods showed fibrillation, higher surface roughness and decrease in density and diameter. Fibers subjected to longer durations and higher concentration of alkaline displayed micro-pores and damages. TGA curves indicated fiber treatment increased the thermal stability and produced less char. DMA studies inferred stiffness and damping properties were better for treated fibers. FTIR studies notified removal of hemicellulose and lignin from fibers

after treatment. XRD patterns displayed the conversion of cellulose I to cellulose II. Mechanical properties improved for less concentration and shorter periods of treatment.

Ferdous et.al. (2014) worked on different weave structure fabrics, tested as per ASTM D5034 and ASTM D5035. The strip test gave better results compared to grab test. Twill weave had better tensile properties than other weave patterns.

Mittal, Saini and Sinha (2016) stated the usage of primary fibers and secondary fibers in processing of composite for minimizing the costs and maximising the properties. Mechanical properties were enhanced by using fillers such as red mud, nano-clay, lignin and clay. Water absorption was hindered by addition of nano-clay. Anti-parallel oriented bamboo represented better tribological and mechanical properties. Alkaline content had more effect on fibers than soaking time on their performance. Agave soaked in alkaline concentration showed better bonding and less water absorption. 1% alkaline treated banana showed 50% improvement in mechanical properties. Alkaline treated coconut sheath increased thermal stability and mechanical properties by 20%. Alkaline treated kenaf showed reduction in damping properties of compostes. Silanized sisal improved flexural properties of grafted rubber. Addition of coupling agents affected tribological, mechanical and thermal properties of jute and basalt composite.

H. Kim et.al. (2013) extracted bamboo by steam explosion and treated with NaOH (1, 2.5, 5, 10%) followed by silane (0.5, 0.75, 1, 2%). TS of alkaline treated fibers was better than other treated ones. IFSS of chemically extracted fiber/epoxy was higher because of lower contact angle and better bonding. Silane treatment improved tensile properties of composites by 37.9% and 47.7% for 1 and 2.5wt%. Water absorption reduced for alkaline/silane treated fibers. SEM displayed matrix cracking in composites due to water absorption.

Porras and Maranon (2012) stacked woven bamboo fabric with PLA. TGA showed that bamboo fabric was stable till 220°C. Tensile studies showed bamboo had higher breaking load along transverse direction than longitudinal. SEM showed crack propagation was perpendicular to loading with fewer fiber pull-outs.

Khan et al. (2011) extracted sisal fibers and treated them with NaOH. TS of 2% NaOH treated fibers was higher with maximum elongation to break. SEM showed the morphological change after treatment improved the wetting and bonding in composites. TGA curves implied higher the concentration of treatment, thermal stability reduced.

Indira et al. (2011) conveyed that banana fibers studied under contact angle measurements had better surface energy for NaOH treated fibers. Alkaline and formic acid treated fibers had better wetting properties compared to untreated. FTIR graphs notified removal of hemicellulose at 1735 cm^{-1} for alkaline treated fibers. SEM showed smooth surface for NaOH treated fibers, removal of wax for acetyl treated fibers and disintegration and fibrillation for benzyl treated fibers. Root mean square (RMS) analysis showed raw fiber had higher surface roughness. IFSS of single bond test showed 17% increase for alkaline treated/PF when compared to untreated/PF. Atomic force microscope (AFM) displayed smooth surfaces for NaOH, silane and formylated treatments. KMnO$_4$ treated fibers had sharp peaks indicating high surface roughness which may lead to better interlocking with resin.

Shah et.al. (2016) stated bamboo fibers extracted by steam explosion had 32.2% lignin. Hydrophilicty of bamboo reduced the bonding capacity with polymers such as rubber, PP and PVC. Bamboo at 0.4 V_f displayed 1.9 times the TS of sisal. Bamboo hybrids showed higher TS and TM compared to pure bamboo composite. Lignin content removal played crucial role in bonding of bamboo with polymer. Fiber morphology and agglomeration limited MAPP as a binder.

Rassiah et.al. (2017) laminated 5 mm width bamboo strips by epoxy. Laminates were prepared by stacking 2 to 6 layers of similar density strips, separately. TS and TM was highest for 2 layered composite which displayed better fracture toughness. FS, FM and impact strength of 2 layered composite was highes. 6 layered composite had highest Shore D hardness.

Rawi, Jayaraman and Bhattacharyya (2013) compressed PLA sheets with plain woven (2/1) bamboo fabric of 35wt% into laminate. DOE results compared were nearer to

experimental values and differences were due to presence of voids or debonding observed under ESEM. Composite showed an improvement of 240% in impact conditions, 240% in tensile and 96% in flexural conditions when compared to neat PLA.

Hybrid Composites

Caldas et.al. (2016) treated banana fibers with sodium carbonate and processed them into laminate by epoxy. Treatment improved TS of banana/epoxy by 79.61% and modulus by 28.01% when compared to untreated banana/epoxy. Banana/epoxy composites at 40 wt% showed highest tensile properties than neat epoxy. FTIR displayed removal of hemicellulose and lignin peaks at 1726 cm^{-1} and 1274 cm^{-1}.

Jawaid, Abdul Khalil and Alattas (2012) sandwiched woven jute fabrics between Oil Palm empty fruit bunch (OPEFB) mat by mixture of epoxy and polyamide in a ratio of 100:60. DMA studies inferred epoxy lost its properties at a faster rate. T_g noticed in loss modulus was higher for jute/epoxy. Peaks observed for epoxy from tanδ curves reduced with fiber addition confirming better adhesion. TGA graphs showed jute/epoxy had highest char residue and sustained for longer time due to presence of cellulose.

Srividya et.al. (2017) worked on long continuous Banana, Americana and Hybrid fibers stacked by epoxy into laminate, separately. TM and FM increased with an increase in V_f and was highest for banana/epoxy at 75% V_f. The experimental values compared with analytical were in par with each other with slight variations for banana fibers.

Meredith et.al. (2012) processed woven flax, jute and chopped strand mat hemp into laminates by epoxy using vacuum assisted resin transfer. Woven fabric composites showed higher tensile properties compared to short and uni-directional fiber composite. Impact test carried under dynamic condition displayed increasing V_f the specific energy absorption increased. Optical micrographs displayed single interlaminar crack formation in flax/epoxy because of higher volume fraction compared to jute/epoxy and hemp/epoxy.

Fuentes et al. (2015) worked on glass fibers treated with piranaha solution and bamboo with warm water for 1hr and then cleaned with ethanol. Surface roughness of bamboo was

higher than glass. IFSS of PVDF is 5 times stronger than PP. Better bonding for glass/PVDF and bamboo/PVDF was because of acidic properties in PVDF and basic constituents present in glass and bamboo. Because of lower properties in transverse direction of bamboo and their anisotropic properties along the length, bamboo/PVDF performed lower than glass/PVDF.

Yan, Chouw and Yuan (2012) treated woven - flax, bamboo and linen with 5% NaOH and piled them into laminate by epoxy, separately. TS of treated flax/epoxy was higher and elongation to break was 50% larger for treated linen/epoxy than treated flax/epoxy. Fiber treatment removed the unwanted impurities such as lignin, hemicellulose and waxes. FS and FM of treated fibers/epoxy was higher than untreated fiber/epoxy.

Mahmud Zuhudi, Jayaraman and Lin (2016) varied the W_f of twill woven bamboo fabric weaved along warp, weft and hybrid sequence and piled them into laminate by PP. Warp sequence showed an increase in TS, TM, FS, FM and impact strength when compared to neat PP. Bamboo increased the thermal stability of neat PP. Maximum deformation of composite was at 40% W_f along the warp direction with higher energy absorption under impact conditions.

Kalusuraman et.al. (2017) treated cocnout sheath and jute fibers by 1N NaOH and later with silanol of 3wt% and 5wt% starch. The fibers were laminated by Isothothalic PE. Hardness, FS and FM were higher for starch treated coconut sheath/PE. ILSS of starch treated hybrid composites was better than untreated hybrid composites.

Ratna Prasad and Mohana Rao (2011) piled unidirectional jowar, sisal and bamboo fibers separately by PE into laminate. TM of jowar/PE at 40% V_f was higher than bamboo/PE and sisal/PE. FS and FM of jowar/PE was better than bamboo/PE and sisal/PE.

Safwan et.al. (2018) analysed woven kenaf fabric, bamboo fabric, bamboo mat and bamboo powder fabricated into laminate by epoxy under compression at 110°C for 10min. TS was higher for bamboo mat/epoxy and TM was higher for kenaf fabric/epoxy. Impact

strength was highest for bamboo fabric/epoxy. SEM showed maximum void presence in bamboo powder/epoxy.

Dash et.al. (2013) compared jute, bamboo and glass mats piled at different orientations by epoxy into laminate. TS was higher for glass/epoxy consisting of fiber oriented in 0°/90° than jute/epoxy and bamboo/epoxy.

Biswas et.al. (2015) piled uni-directional jute and bamboo fibers separately by epoxy into laminate under vacuum. TS and strain to failure was higher for bamboo/epoxy and young's modulus was higher for jute/epoxy. SEM showed the amount of fiber pullout for bamboo/epoxy was higher than jute/epoxy. FS and FM was higher for bamboo/epoxy. Jute/epoxy failed parallel to loaded direction and bamboo/epoxy failed perpendicularly. FS and FM of jute/epoxy was 2 times that of bamboo/epoxy in transverse orientation. TGA showed jute/epoxy had better thermal stability than bamboo/epoxy.

Singh, Kumar and Srivastava (2018) performed tensile, impact, hardness and buckling tests on cross-woven glass fibers reinforced composites. TS was highest for composite of 4.4mm thickness and 5 wt% cement. Thickness effect reduced crack initiation. More than 1wt% cement in composite reduced the impact properties due to agglomeration. With 5wt% cement, composite of 6.3 mm thick had highest critical buckling. SEM images displayed change of cracks path in composite due to the presence of cement.

Deepak et.al. (2017) treated jute fiber mats with ethanol and fabricated them into laminate by epoxy + polyamide (PA) and phenalkamine hardeners separately. Tensile properties of composites consisting mixture of PA and PKA at a ratio of 50:50 gave better results. Flexural properties were better for epoxy/polyamide composite. Impact properties were better for epoxy/PKA composite. HDT analysis showed epoxy/PKA had better resistance to humid conditions.

2.3 Epoxy/Phenalkamine Polymer Composites

Panda et.al. (2015) compared mechanical and wear properties of phenalkamine (PKA)/epoxy and polyamine (PA)/epoxy. TS of epoxy/PA was higher than epoxy/PKA,

but elongation to break of epoxy/PKA was higher. Impact properties were higher for epoxy/PKA compared to epoxy/PA. Wear properties showed higher values for epoxy/PKA compared to epoxy/PA.

Benega, Raja and Blake (2017) tried curing of epoxy with different types of hardeners produced from cashew nut shell liquid (CNSL) and compared with conventional hardeners. Presence of an aromatic ring and aliphatic chain in CNSL hardener made them resistant to fire and chemicals. Post curing of matrix showed enhancement in young's modulus and water resistance for CNSL derived hardeners.

Mustapha Razak and Abdul (2018) worked on montmorillonite (MMT) nanoclay mixed with epoxy and PKA. The TS and FS of epoxy improved with addition of MMT at 0.5phr and reduced further due to agglomeration or non-uniform dispersion of clay. FM of composite was higher at 1phr compared to neat epoxy. Impact strength reduced with addition of MMT in composites. TGA showed better thermal resistance for 0.5phr/epoxy. Water absorption was low at 0.5phr MMT and increased further with the addition of MMT.

2.4 Influence of weave pattern and thickness of composite

Rassiah et.al. (2017) laminated 5 mm width bamboo strips by epoxy. Laminates were prepared using 2 to 6 layers of similar density strips. TS and TM was highest for 2 layered composite in which failure propagated from matrix to fibers and displayed better fracture toughness. FS, FM and impact strength of 2 layered composite was highest and failure propagated from the cracks developed. 6 layered composite had highest Shore D hardness.

Dhakal and Keerthi Gowda (2017) mixed banana fibers with PE and processed the mixture into laminate. TS increased with an increase in V_f and thickness of the composite. FS increased with an increase in fiber length, V_f and thickness of composite. Impact properties enhanced with thickness of composite and V_f.

Krishna Adhikari and Keerthi Gowda (2017) processed banana and jute fibers in ratio of 1:1 and piled them into laminates by Polyester (PE). TS was highest for 5 mm thick and 15% V_f composite. Impact strength was highest for 25% V_f and 5 mm thick composite.

Singh, Kumar and Srivastava (2018) performed tensile, impact, hardness and buckling tests on cross-woven glass fibers reinforced composites. TS was highest for composite of 4.4 mm thick at 5 wt% cement. Impact properties reduced for more than 1 wt% cement in composite, due to agglomeration. With 5 wt% cement, composite of 6.3mm thick had highest critical buckling. SEM images inferred change of cracks path in composite was due to presence of cement.

Alantali et al. (2018) fabricated a 3D glass-fabric composite by vacuum assisted resin transfer molding. The resin flow took time with an increase in the number of layers and flexural results increased with an increase in thickness of composites.

Alavudeen et al. (2015) worked on woven and random banana/kenaf composites. The TS, FS and impact strength was higher for plain woven hybrid composites than twill woven hybrid. An increment in results for sulphate treatment was due to better bonding with reinforcement compared to NaOH treatment and untreated.

Hanamanagouda et al. (2016) concluded that increasing the V_f of randomly oriented jute/PE composites has an impact on mechanical properties, whereas thickness has minimal effect.

Hartoni et al. (2017) studied the effect of skin thickness and core thickness of bamboo composites on flexural properties. The flexural strength increased with core thickness and was higher for 6 mm skin thickness and 7 mm core. The failures observed indicated separation of core from the skin without any damages.

Nayeem Ahmed and Salman Mustafa (2015) fabricated hybrid composite of carbon-glass-grpahite, which showed reduction in tensile results and an increase in compressive results with varying thickness of composites.

Swamy, Patil, & Chame (2016) showed 1-directional glass/epoxy performed better than bi-directional woven glass/epoxy and 2-directional glass/epoxy under flexural conditions. With an increase in thickness the flexural properties also improved and the results were higher for 6 mm thickness composites.

2.5 Conclusions from Literature Review

From the abundant literature available on different forms of natural fiber reinforced composites and matrices, one can observe the following:

1. The findings from literature review infers about poor interfacial bonding between the natural fiber and matrix due to hydrophilic nature of fiber, fiber surface roughness, polar groups on fiber surface, surface energies, wetting angle and incompatibility of bonding with matrix.
2. Few solutions such as alkaline treatment, use of coupling agents and coating on fibers are suggested by researchers. Treatments have improved the permeability properties of fiber and bonding between fiber and matrix in composites.
3. Phenalkmine hardeners known for moisture resistance have shown better impact properties at lower values. From the literature review, it can be concluded that enough work has not been carried out on characterisation of composites made of low aerial weight bamboo fabric with varying thickness using phenalkamine hardener as curing agent for epoxy.

2.6 Objectives

1. To prepare and process the natural fiber reinforced composite using 125gsm low aerial weight Plain and Twill Weave Bamboo Fabric and Epoxy B-11 resin with AI 1041 phenalkamine hardener
2. To determine the influence of raw fabric weave pattern and thickness of composite on
   a) Static and dynamic mechanical behaviour of bamboo reinforced composite
   b) Flammability and water absorption behaviour of bamboo reinforced composite
3. Thermal characterization of raw fabric and raw bamboo fabric reinforced composite

2.7 Methodology

Raw Materials for Project

Natural Fibers
Bamboo (plain & twill)

Reinforcement

Matrix

Thermoset
Epoxy B-11/ AI 1041
        Phenalkamine

Testing
1. FTIR – Presence of cellulose, lignin
2. XRD – Amorphous and crystalline nature
3. Strip Test of fabrics
4. TGA
5. DSC

Testing
1. FTIR

Laminate (Plain || Twill)
Plain weave of 3, 4 and 5 mm thick
Twill weave of 3, 4 and 5 mm thick

Mechanical Testing – Tensile, Izod, Flexural

Characterization
SEM

Thermo-mechanical Testing – DMA

Water absorption studies

Flammability studies

Thermal testing – DSC, TGA

Chapter 3

EXPERIMENTAL DETAILS

In this chapter, the materials utilized, the fabrication process and the testing conducted on the composites have been discussed

3.1 Materials

Material	Properties
Bamboo Fabric (Plain and Twill weave)	125 gsm, 2/30 X 2/30 yarn count
Epoxy Resin (B-11)	1.15-1.18 g/cm3, 11000-15000 mPas @ 25 ⁰C
Phenalkamine hardener (AI 1041)	0.98-1.0 g/cm3, 20000-50000 mPas @ 25 ⁰C

3.2 Fabrication of Composite

- Plain and Twill weave fabric were cut into 200 X 300 mm^2 dimension along warp direction for layup
- Wax and Over Head Protective (OHP) sheets were used as releasing agents or peel ply
- Metal Pad was used for wet layup, a glass stirrer was used for mixing of resin and hardener in a fiber beaker
- Ceramic tiles were used as moulds to achieve smooth finish and aluminium strips were used as spacers to achieve the required thickness
- Mould was prepared by cleaning the surface with acetone and then applying wax on the surface
- The OHP sheets were cleaned with acetone and wax was applied on both sides of the sheet
- Resin and hardener were added in equal ratio as suggested by the industrial operator and was thoroughly mixed at a pace
- The wax coated OHP sheets were placed on the mould

- A defined amount of matrix was poured on to the sheets and was spread evenly all over the surface

- A layer of cut fabric was placed on the evenly spread matrix

- Over it the matrix was poured once again which was distributed all over the fabric using a metal pad

- Similarly, the composite fabrication was operated till the required thickness was achieved

- 50% Fiber volume fraction ratio was maintained to get the required thickness

- For 3 mm thickness layup, 5 layers of fabric were piled

- For 4 mm thickness layup, 7 layers of fabric were piled

- For 5 mm thickness layup, 9 layers of fabric were piled

- After achieving the required thickness another mould was placed on it and uniform load was kept over the mould to remove excess resin

- It was left to cure for 24 hours and was removed easily

- The peel plys (OHP sheets) and wax helped in achieving easy removal of composites and achieve a better surface finish

- Cutting of composites was done on conventional cutting machine

3.3 Characterisation

3.3.1   Fourier Transform Infra-red (FTIR)

Organic and inorganic compounds present in the samples were determined by FTIR. The infrared passed through the sample was recorded as absorption or transmittance. The recorded result will be plotted on graph through which the presence of functional groups will be determined. Each group has a unique wavelength which makes it easily identifiable in the output spectrum. The wavelength was transmitted within range of 4000 cm^{-1} and 400 cm^{-1}. The output obtained from the sample was analysed and displayed in a single beam. The concentration of a particular group was identified from the area under the curve. There are two types of testing, a) Attenuated total reflectance method b) Transmission c) Specular

reflection and d) Diffuse reflectance. Specimens need to be thin such that the infrared can pass through it, thicker specimens have not been suggested.

Three samples of fabric, resin and composites were prepared in small flakes and were tested. FTIR analysis was carried out using a Jasco FTIR-4200, Japan equipment. The spatial resolution was set at 4 cm^{-1} and scanned between the spectral bandwidth of 4000 - 400

cm^{-1}. The testing procedure was carried as per Attenuated Total Reflection (ATR) method in which the sample will be bombarded with infrared beam and the functional groups absorbed some amount of IR beam resulting into a spectrum.

3.3.2 X-Ray Diffraction (XRD)

As the interatomic spacing is 2-3 Å, XRD has been chosen as a non-destructive method to identify an unknown crystalline structure in the sample, presence of minerals, purity of sample and so on. Thin samples of 1-2 mm thickness either in liquid, powder or solid form have been suggested for testing. A monochromatic beam of X-rays was impinged on the sample between angles 10 - 80⁰ and the reflected beam was recorded and plotted on the graph. A pure crystalline material was indicated with a sharp peak, whereas an amorphous or semi-crystalline material shows a broad curve with a maximum intensity.

XRD analysis of fabric was carried out on a Malvern Panalytical X'Pert[3] Powder Diffractometer equipment. Small pieces of fabric were cut in 2 X 2 cm^2 size and subjected to a wavelength of Cu-Kα (1.54A⁰) by varying the angle from 0⁰ to 80⁰ at rate of 2⁰/min.

3.3.3 Strip testing of fabrics

As suggested by Ferdous et al. (2014), the fabrics were prepared according to ASTM D5035 - 2R – 65 mm raveled strip test, with gage length of 75 mm, total length of 280 mm and width of 65 mm as show in **Fig. 3.1**. Five samples of fabric were cut along the warp direction and five samples along weft for both plain and twill weave fabric. All the samples were raw fiber fabrics which have not been subjected to any treatment. The cut samples were kept in an air tight bag to avoid any moisture absorption before the testing. The fixtures used for fabric testing were square metal clamps, parallel to each other and

smoothly finished. The experiment was conducted on ZWICK//ROELL Z020, LOADCELL 20 kN, with a cross-head speed of 300 mm/min.
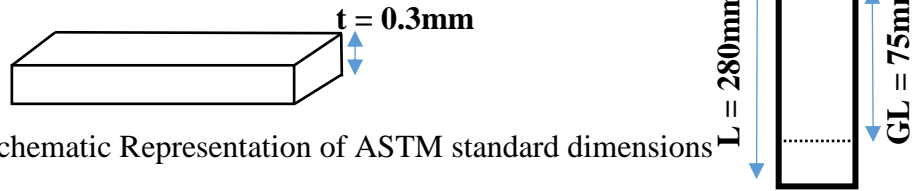
Figure 3. 1: Schematic Representation of ASTM standard dimensions
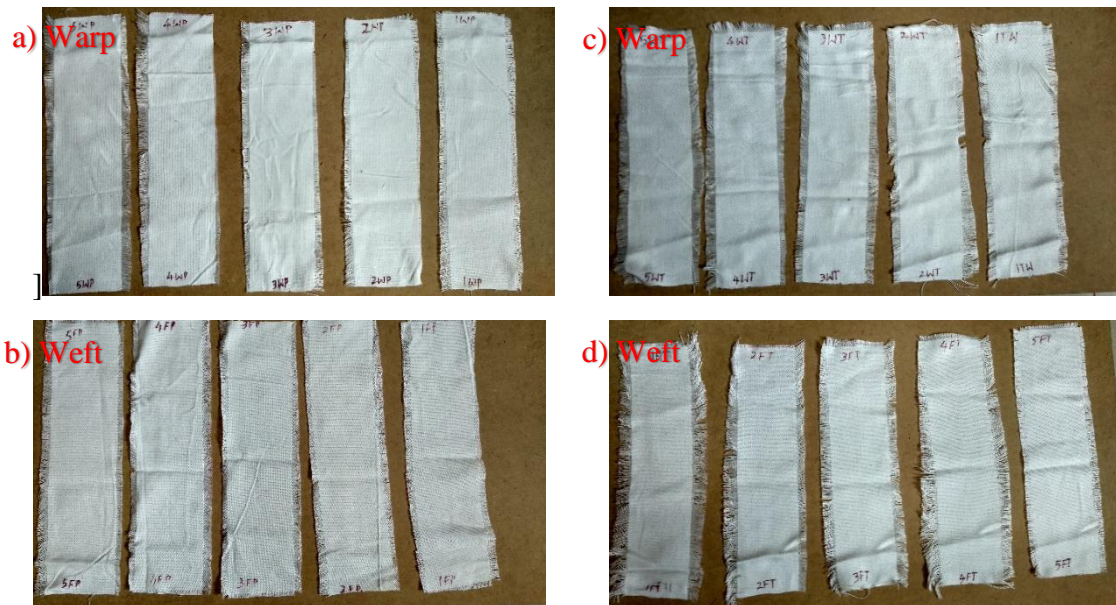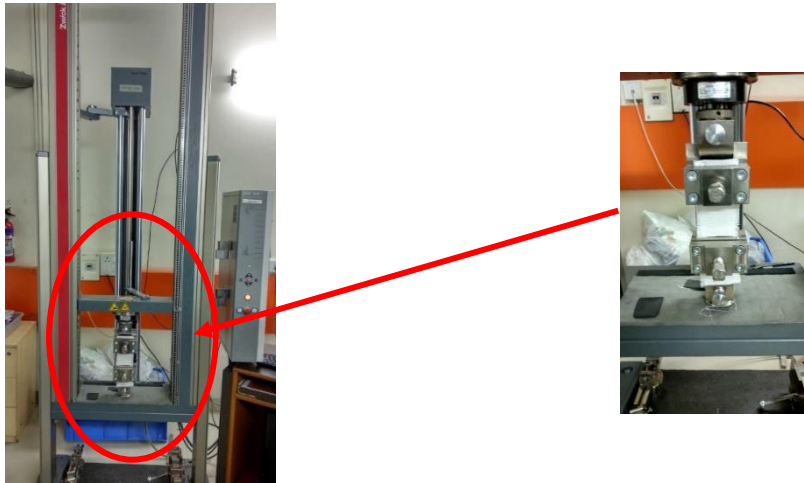
Figure 3. 2: Strip testing of fabrics, a|b) Plain weave fabric, c|d) Twill weave fabric

3.4 Mechanical Testing and Fractography

3.4.1 Tensile testing of composites

The experiment was conducted on ZWICK//ROELL Z020, LOADCELL 20 kN, with a cross-head speed of 2 mm/min as per ASTM D3039 considering balanced and symmetrical fibers i.e. for woven fabrics as show in **Fig. 3.2**. Five Specimens of both plain and twill weave composite were cut by conventional cutting machine. Length of specimen measured after cutting was 250 mm, breadth was 25.4 mm and thickness. The naming of specimens was done by first the thickness of specimen, second was weave pattern and third was specimen number. For e.g. 3P1 means 3 mm thickness, P is plain weave and 1 was specimen number. Due to smoothness of the specimen there was slippage observed in initial trail runs. Sand papers of 100 gsm were used to hold the specimens tightly in the fixture as suggested in ASTM D3039.
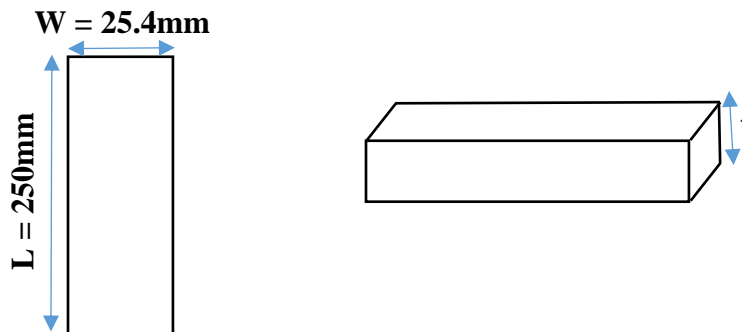
Figure 3. 3: Schematic representation of ASTM D3039 standard dimensions

Calculations

Stress (σ) = Load (P) / Area (A)   (3.4.1.1)

Young's Modulus = $\Delta\sigma / \Delta\varepsilon = \sigma_2 - \sigma_1 / \varepsilon_2 - \varepsilon_1$ (3.4.1.2)

Strain (ε) = Change in length (ΔL) / Original length (L_o) = $(L - L_o) / L_o$ (3.4.1.3)

Stiffness (k) = Change in force (Δf) / Change in deflection (Δx) (3.4.1.4)

Density (ρ) = Mass (m) / Volume (v)   (3.4.1.5)
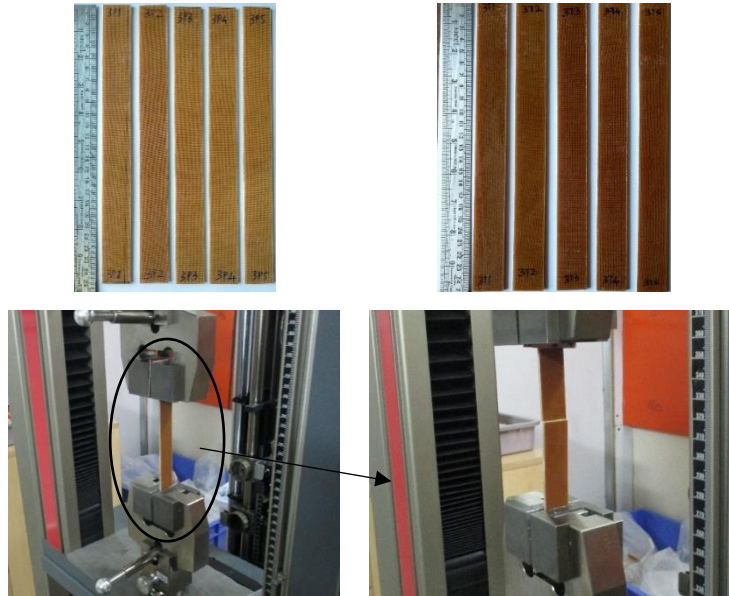
Figure 3. 4: Tensile testing of PWC and TWC

3.4.2   Flexural testing of composites

The tests were conducted as per ASTM D790 standard as show in **Fig. 3.3**. 5 specimens were cut conventionally with dimensions 13.4 mm breadth, 127 mm length and thickness. The cross-head speed was calculated based on the equation as below
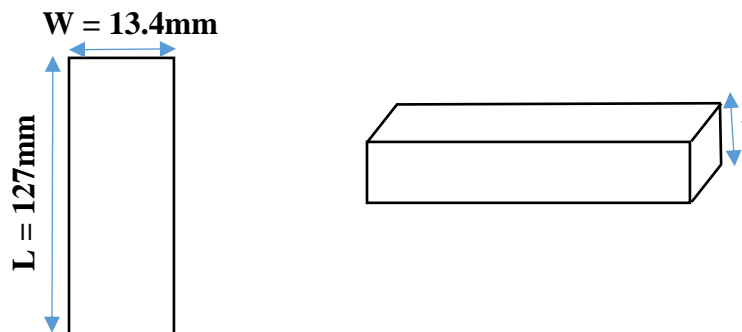
Figure 3. 5: Schematic representation of ASTM D790 standard dimensions

$$R = \frac{ZL^2}{6D}$$ (3.4.2.1)

Z = strain rate 0.01, L = span length (mm), D = beam thickness (mm) and R = rate of crosshead (mm/min)

The flexural strength was calculated as per below equation

$$\sigma_f = \frac{3PL}{2BD^2} \quad\quad\quad (3.4.2.2)$$

P = load in newton (N), L = span length mm, B = width (mm) and D = thickness (mm)

The flexural modulus or chord modulus was calculated as per below equation

$$\epsilon_f = \frac{6Dd}{L^2} \quad\quad\quad (3.4.2.3)$$

where D = maximum deflection at centre (mm), d = thickness (mm) and L = span length (mm)
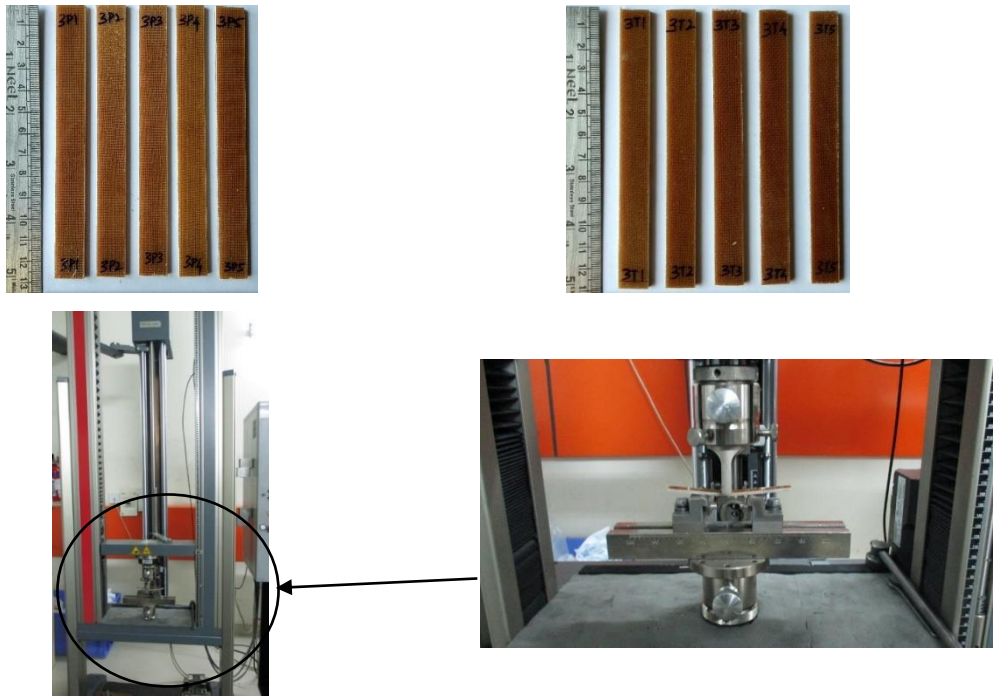
Figure 3. 6: Flexural testing of PWC and TWC

3.4.3 Izod Impact testing of composites

Impact testing of composites were carried out as per ASTM D4812-99 standards using a ZWICK /ROELL HIT 50P as shown in **Fig. 3.4.** The nominal work capacity was 5.5J and impact velocity was 3.458 m/s. The specimens were cut into 63.5 mm length X 12.7 mm width X thickness as per ASTM standards. A centre line was marked on the specimens &

placed such that the centre line divides the specimen into two halves where the first half will be in the anvil and the other above the anvil. The hammer was held at distance from the centre of the machine. After the specimen was placed on the machine, the value was set at zero and then hammer was released from the rest position. The hammer moves along the arc of radius and hits the specimen at the top half causing an impact on the material. Then the hammer was brought back to normal position after the momentum slowed down. The reading was noted from the digital indicator.
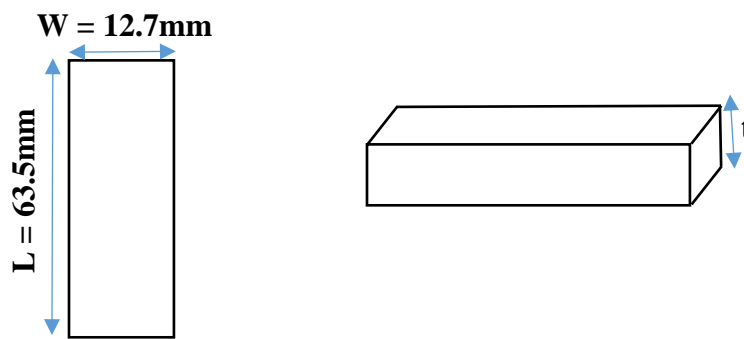
Figure 3. 7: Schematic representation of ASTM D4812-99 standard dimensions
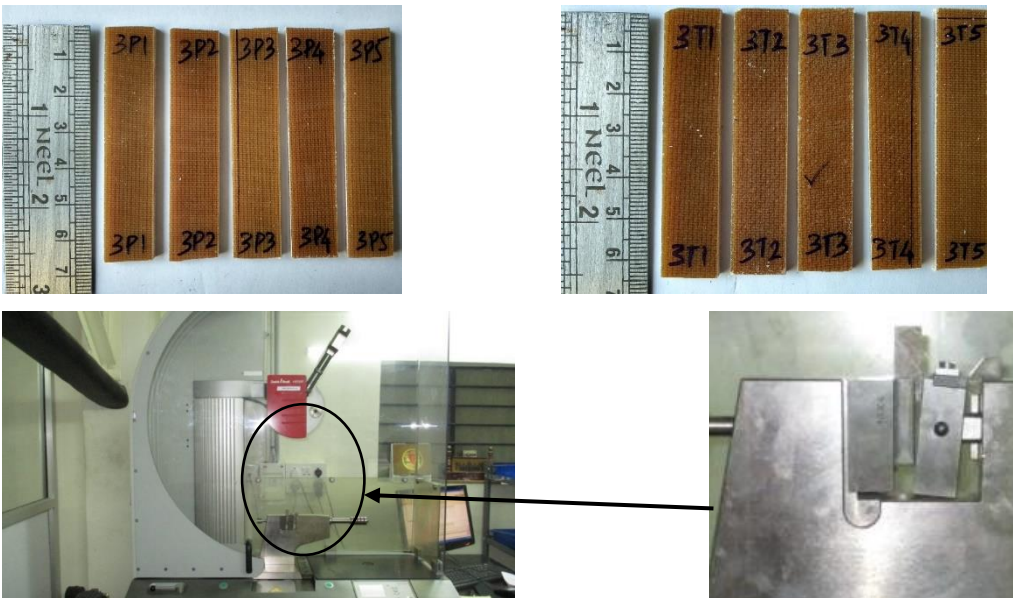
Figure 3. 8: Izod impact testing of PWC and TWC

3.5 Fractography of tensile tested specimens

The analysis is done on TESCAN VEGA3|LM machine shown in **Fig. 3.5**, has 5-axis motorized holder. It has resolution till 30 KV and magnification of 100000x which can be

used to analyse even at nano level. The electron gun was a tungsten heated cathode which bombards the electrons over the sample. There are two types of specimen's i.e conductive and non-conductive materials. For conductive materials the specimens were loaded into the chamber as received. They must have better surface finish else polishing of surface was required. For non-conductive materials coating needs to be done. As shown in the image a sputtering machine was used for coating a gold film over the specimen to avoid the exciting of specimen. The coating was conducted by placing the specimen into the cylindrical box, later the degassing of material was done to remove any air or moisture present before coating. Then plasma was generated which passes to the target at 90º between the magnetic lines formed. A smooth coating of gold was achieved at rate of 10 nm/m. After coating the specimens, they were loaded into the SEM machine and nitrogen gas was used to pressurize the chamber. After the chamber had achieved the required pressure, scanning of specimen was performed.

Figure 3. 9: SEM instrument and Plasma coating apparatus

Fractured specimens from tensile test were examined on Scanning Electron Microscope (SEM) - TESCAN VEGA3 AMU equipment at an operating voltage of 10 kV. The tensile tested specimens were coated with gold, by sputtering method and were kept in the

equipment under vacuum for failure analysis. The surface of the failure and the top flat surface were magnified between 50X – 800X magnification to determine the failure.

3.6 Thermal testing

The type of sample can be solid or liquid, but not gas. Absolute or difference in property to the referenced or the rate of change of property with temperature i.e. derivative, was recorded for analysis purpose. Sophisticated instruments provide qualitative and quantitative details about the materials subjected to heat variations. Different type of testing such as TGA and DSC have been carried out for analysing the material behaviour subjected to temperature variations. A perfectly crystalline structure solid was considered as a reference and as real solids have imperfections, the difference was observed. Glass transition temperature defines a time interval where the material becomes flexible, for analysis only the peak of the time interval has been considered. Heating causes vibration in the lattice constants leading to phase transitions, melting, sublimation and thermal degradation (Simon 2005)

3.6.1   Thermo-Gravimetric Analysis

The sample was placed in a controlled environment and was weighed continuously along time while it undergoes heating and cooling. Using an electro-optical device, the sample was placed at null-point. The variation in the weight alters the balance beam, indirectly altering the light intensity, thus the difference was recorded. The furnaces compromising of electrical resistive heaters to reach a temperature of 1000 ºC and for high temperature radiations. An atmosphere with inert gases has to be maintained to minimize reactions, remove corrosive products and act as coolant. Thermocouples used must be of small diameter to measure sensitivity, though large diameter are preferred due to their longevity, they lack sensitivity compared to small ones. There are two types of heating a) linear when the temperature varies with time and b) isothermal to keep the temperature same for longer duration.

In present work samples have been prepared in a form of small flakes as the pan used for testing is about 2-3 mm. The fabrics from plain and twill weave were cut into small flakes and were packed in an air tight bag as three different samples. Plain weave composite (PWC) and Twill weave composite (TWC) of 3.1, 4.3 and 5.4 mm thickness were cut along the surface to get samples in flakes form and were placed in an air tight bag as three different samples. The samples were further tested on Perkin Elmer TGA4000 instrument **Fig. 3.6,** KONSPEC Mangalore, by subjecting to temperature range from 25 ⁰C to 700 ⁰C. Heating was maintained at 10 ⁰C/min. Nitrogen atmosphere was maintained at 50 ml/min.
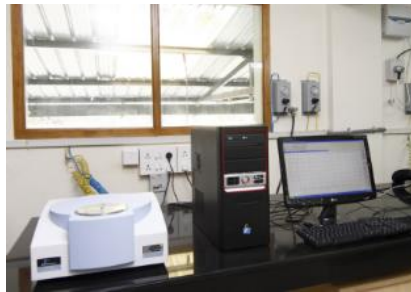
Figure 3. 10: TGA | DSC instrument

3.6.2 Differential Scanning Calorimeter

The measurement of heat variation in sample body with reference was analysed to determine the phase transitions, purity determination, material characterization and melting. Heat flux and Power compensated DSC are two types of measuring devices. In heat flux DSC, when the heat flows over the sample the differential temperature will be maintained at zero, any variation or transitions occurring was measured by thermocouples. In power compensated, electric energy was supplied in form of heat as a compensation to heat variation, thus the temperature difference was the heat supplied. The temperature difference was given as output in form of voltage. Endothermic curves were observed for samples consuming heat for breaking of bonds and it was pointed upwards and exothermic curves were observed downwards when heat was released due to reactions.

In present work samples have been prepared in form of small flakes as the pan used for testing is about 2-3 mm. The fabrics from plain and twill weave were cut into small flakes and were packed in an air tight bag as three different samples. PWC and TWC composites

of 3.1, 4.3 and 5.4 mm thickness were cut along the surface to get samples in flakes form and were placed in an air tight bag as three different samples. The samples were further tested on Perkin Elmer DSC6000 instrument **Fig 3.7,** at KONSPEC Mangalore, by subjecting to temperature from 25 ⁰C to 400 ⁰C. Heating was maintained at 10 ⁰C/min. Nitrogen atmosphere was maintained at 50 ml/min. The results have been displayed in **Table 5.2.**

3.7 Dynamic Mechanical Analysis (DMA)

DMA was imported from field of rheology as it deals with deformation and transitions happening with the material. Compared to stress-strain curve obtained from mechanical testing, here a modulus was obtained by applying a sine wave across sample through temperature or frequency sweep. Three energies have been notified from DMA, a) store energy, b) lost energy and c) damping. Compared to young's modulus, storage modulus was determined from a point on line subjected to oscillation under temperature sweep. Storage modulus an in phase modulus has been also called as elastic modulus. Loss modulus also known as viscous modulus an out of phase modulus and it shows the amount of energy lost. Both these modulus have been dependent on geometry of material. The damping tanδ, a ratio of loss to storage modulus has been independent of geometry and indicates the material behaviour due to internal friction and molecular rearrangements. In temperature sweep the sample was subjected to varying temperature under constant frequency, whereas for frequency sweep its vice-versa. As the test begins from low temperature the molecules were held tightly, thus the sample goes through solid-state transitions. Further increasing the temperature, movements among the local bonds and side chains lead to gamma transition, some toughness was observed at beta transition. T_g was observed after beta transition only for amorphous materials and not for crystalline. Finally the melting was observed during material flow due to large-scale chain slippage, if the material was thermoset then slippage was not observed as the cross-linking prevents the chains from doing so. T_g also defines the operating range of material. Rubbery region

defines the crystallinity of material and also the number of cross-linking in the material (Menard 1999).

Three samples of plain and twill weave composite of varying thickness were tested on TA Instruments Q800 **Fig 3.8**, by mounting on a dual-cantilever beam testing machine as per ASTM D5418-01. The amplitude was set at 10 µm and 1 Hz frequency. The heating rate was set at 3 ⁰C/min, heating range from 25 ⁰C to 180 ⁰C.
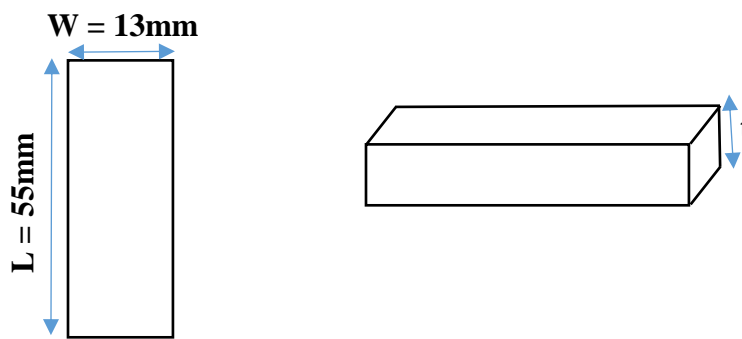
Figure 3. 11: Schematic representation of ASTM D5418-01 standard dimensions
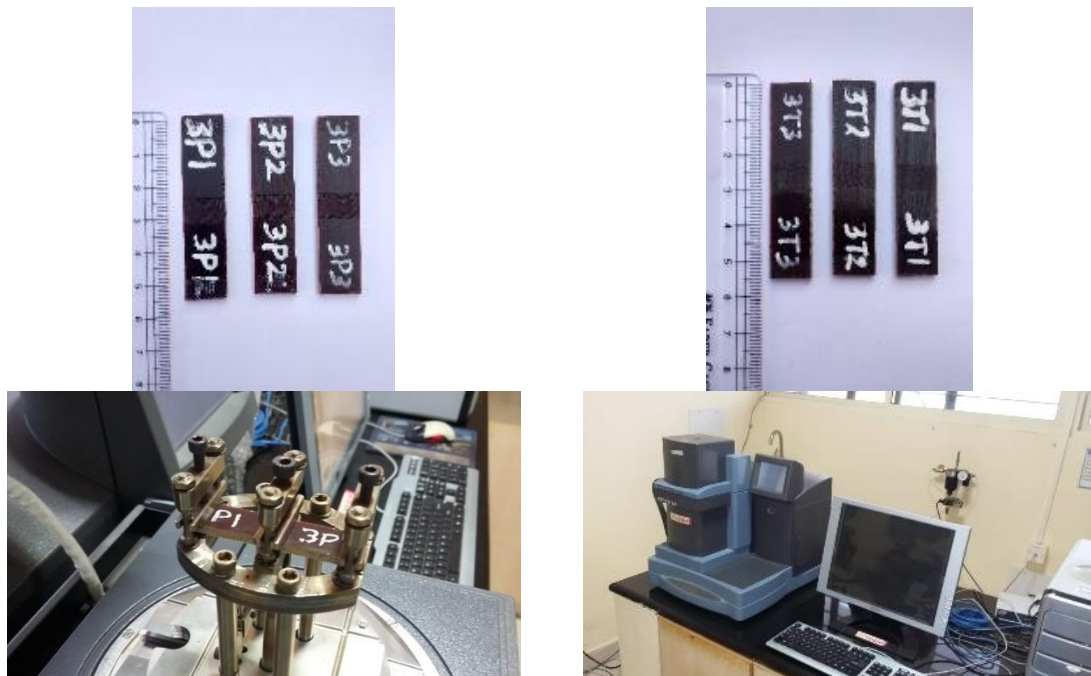
Figure 3. 12: DMA testing of PWC and TWC

3.8 Water absorption and Flammability

3.8.1   Water absorption

Swelling has been considered as a predominant factor in water absorption because it leads towards degradation. Swelling also leads to hygral stresses developed due to hindrance in expansion of composites. The water flow was governed by diffusion and percolation such that it passes through gaps and cracks present in the composites. Water molecules randomly transfer from higher concentration to lower, through diffusion. Whereas percolation, a slow process of water transfer occurrs when the reinforcement content was below threshold level. Absorption of water changes the behaviour of composites because it affects the structure of fiber, matrix and the interface (Väisänen et al. 2017). The hydroxyl groups present in fiber have an affinity towards absorption and the amorphous regions namely hemicellulose and semi-crystalline cellulose also get involved in absorption. Whereas lignin having low carbon to hydroxyl group ratio, acts as hydrophobic. Due to leaching of water soluble substances, osmotic pressure pockets develop at fibre surfaces leading to cracks and de-bonding. This leads to poor transfer of load between the interfaces, thus resulting in reduction of mechanical properties. To curb the water absorption fibre treatments, hybridization, coatings and so on have been studied (Mochane et al. 2019)

Five specimens of plain and twill weave composite of varying thickness were kept in salt water (S) and distilled water (D). The testing was done as per ASTM D570-98 standard as shown in **Fig. 3.9**. The specimens were weighed before immersing into the water and the measurements were noted in weights i.e. grams (gms). Then the specimens were kept in water and the weights were measured consecutively after immersing for 2, 6, 12, 24, 48, 72, 96, 120, 144 hours.
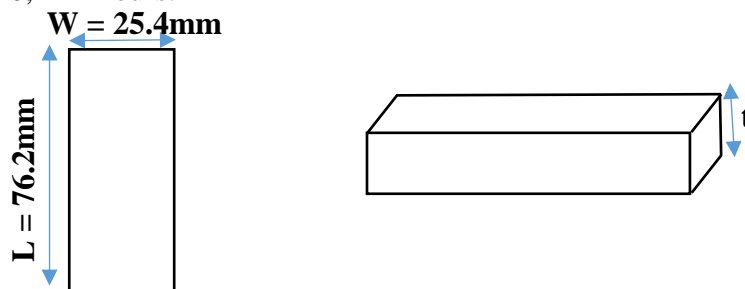
Figure 3. 13: Schematic representation of ASTM D570-98 standard dimension
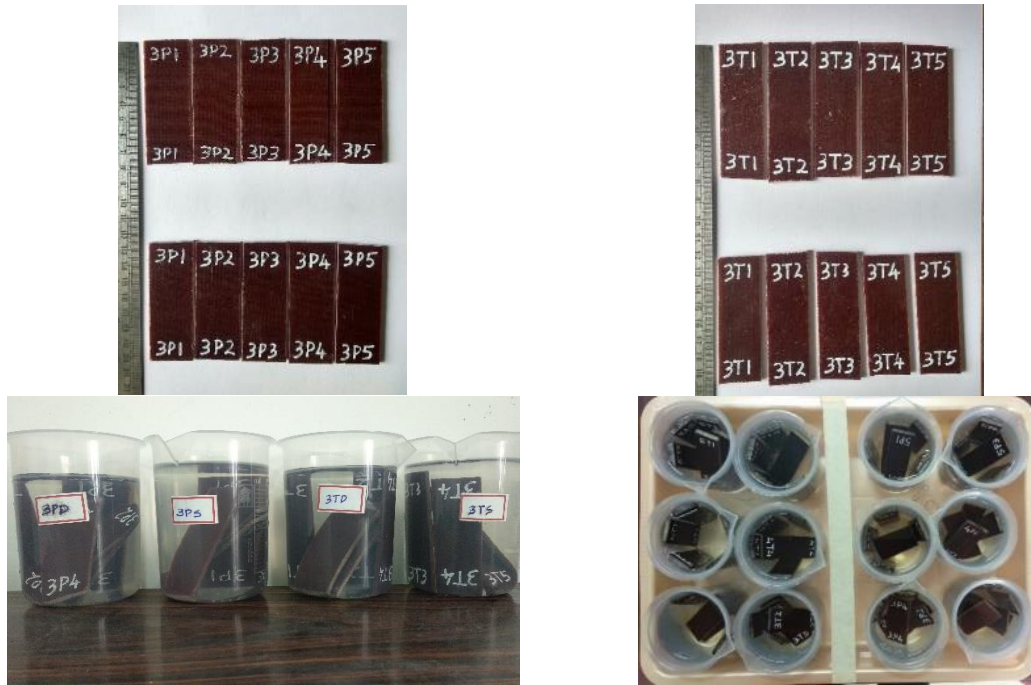
Figure 3. 14: Water absorption testing of PWC and TWC

3.8.2 Flammability

The reinforcement and matrix behave differently when subjected to burning by releasing gases and smoke. The initial stage of burning has been ignition which can prevail over longer period with high amount of gases or for lower periods with high heat release. The volatiles produced vary w.r.t the polymer and if they come in contact with oxygen it leads to burning and decomposition. Crystallinity and orientation have an effect on flame retardancy. Increase in fiber volume fraction and thickness also reduce flame burning rate. Layer by layer burning has been observed in composites such that after the first layer, the heat travels to adjacent layers where the decomposed products move to burning zone through char. Flame retardant were used in thermosets, whereas dripping reduces burning rate in thermoplastics (Campbell 2010)(Fan and Fu 2016).

Three samples were subjected to flammability test as per UL-94HB horizontal burning standards on ATLAS HVUL2 equipment as shown in **Fig. 3.10**. The specimen was marked at 25 mm and 100 mm along the length. The flame was ignited from burner inclined at 45º to the horizontal specimen. The burner was placed at 2 mm distance below the sample tip

marked at 25 mm end. After the flame reaches the 25 mm mark, the timer starts and the readings were noted until the flame reaches 75 mm and the timing was noted down in seconds. The burning rate was calculated as per standard equation $V = 60L/t$, where $V =$ burning rate in mm/min $L =$ burned length in mm, $t =$ time in seconds.
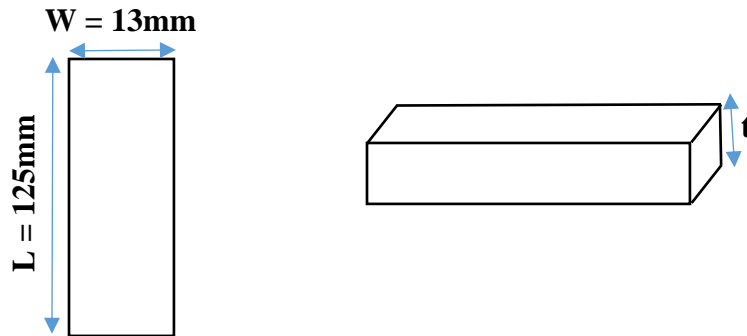
Figure 3. 15: Schematic representation of UL-94HB standard dimensions
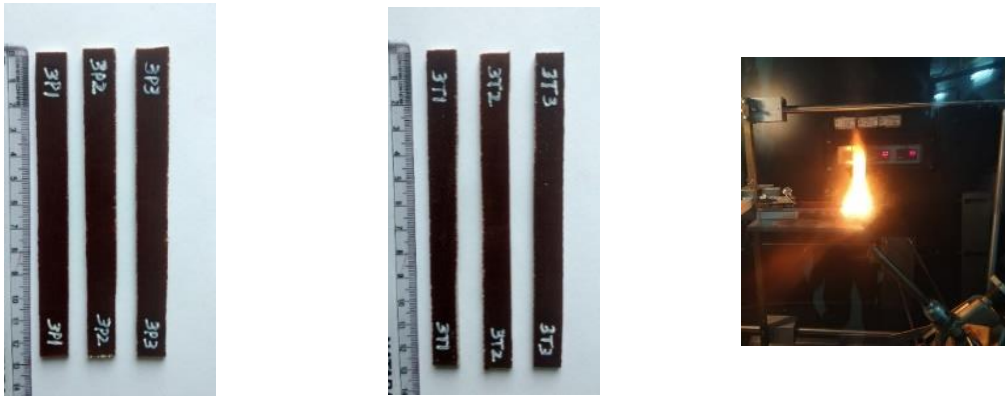
Figure 3. 16: Horizontal burning of PWC and TWC

CHAPTER 4

RESULTS AND DISCUSSION – CHARACTERIZATION

In this chapter, basic characterization of the specimens done in order to determine the presence of moisture and bonding sites, the amount of area available for bonding and strip testing of reinforcement carried out to determine its strength and modulus have been discussed.

4.1 Fourier Transform Infra-Red (FTIR) Analysis

Fig. 4.1 displays a peak at 1166 - 1160 cm^{-1}, related to C-O-C stretching of glycosidic linkage, indicating the presence of cellulose in fiber (Kiew Liew et al. 2017). A broad peak of O-H stretching of hydroxyl groups was noticed at 3600 - 3000 cm^{-1} and a small peak of C-H stretching of cellulose and hemicellulose was noticed at 3000 – 2900 cm^{-1} (Sathish et al. 2017, Ghaedi et al. 2017) .At 1370-1300cm^{-1} the bending vibration of C-H and C-O was due to aromatic rings present in polysaccharides (Sathish et al. 2017) (Ghaedi et al. 2017). Presence of water was determined at 1651 – 1646 cm^{-1} by H-O-H stretching in bamboo (Kiew Liew et al. 2017). Peaks at 1240 cm^{-1} and 2854 cm^{-1} were attributed to stretching of C-N of aliphatic chain and C-H of its side chain, indicating the presence of cardanol in the matrix (Joy et al. 2015, Pathak and Rao 2006). At 1650 cm^{-1} presence of wax was defined due to vibration of C-O group (Costa Júnior et al. 2015). Peaks observed at 2854 cm^{-1} in resin was due to C-H stretching of side chain present in cardanol (Joy et al. 2015). The shift in the wavenumber at 3340 – 3380 cm^{-1} in composites was due to hydrogen bonding (Abdul Khalil et al. 2018).
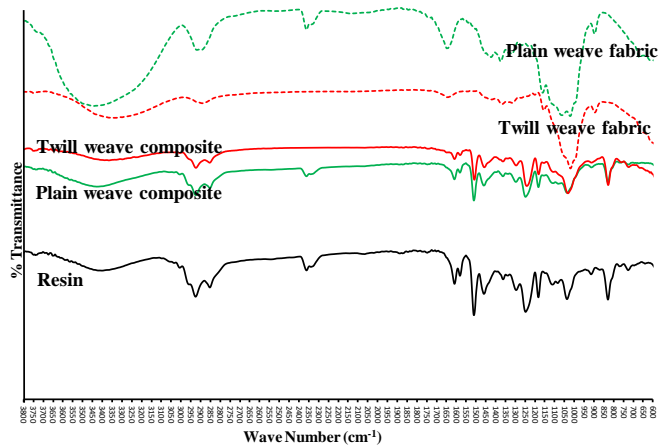
Figure 4. 1: FTIR analysis of bamboo, composite and neat resin

4.2 X-Ray Diffraction Analysis

Fig. 4.2 shows a continuous curve representing an amorphous hemicellulose with lower peaks and cellulose with the higher peaks. The crystallinity index was determined from (Segal et al. 1959) method, considering crystalline peak at 21.3065º and amorphous peak at 13.115º. The crystallinity index determined was 67.85% for twill weave and 67.17% for plain weave (Park et al. 2010). Higher intensities of twill weave indicate presence of more cellulose for bonding.
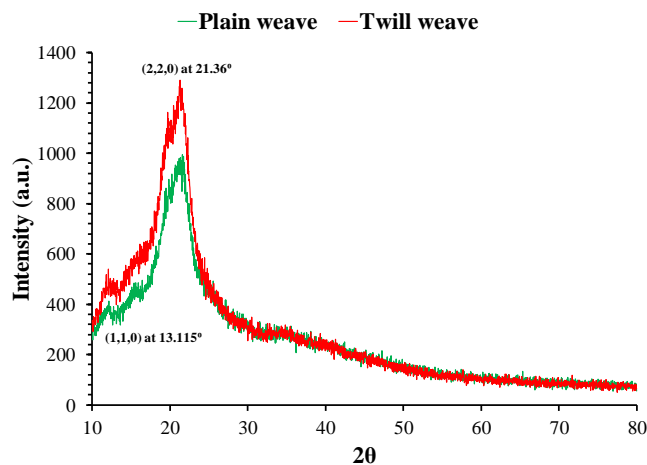
Figure 4. 2: XRD Analysis of plain and twill weave fabric

4.3 Tensile studies of fabric

Table 4. 1: Values determined from Strip test of bamboo fabric

Fabric	Warp Plain weave	Weft Plain weave	Warp Twill Weave	Weft Twill Weave
Average of Max. Breaking Force (N)	653.298	592.461	653.877	568.871
Ultimate Tensile Strength (MPa)	33.502	30.382	33.532	29.173
Young's Modulus (GPa)	0.155	0.147	0.157	0.135
S.D	1.57	1.57	1.16	1.22

The initial curve formed was due to looseness of fibers aligned in pattern, once the resistance of aligned fibers starts, a sudden rise in curve was observed and it saturates later. The middle portion was the elastic region of the fibers which reaches the maximum strength after which it fails. From the results it can be inferred that ultimate tensile strength was higher in warp direction than weft, because during weaving the yarns in warp direction were held in tension whereas the weft was weaved along transverse direction. Thus the tensile strength of fabric in warp direction was always greater. The average values infer that twill and plain weave fabrics have similar performance under tension. And the fabrics possess better properties along warp direction than weft as observed from **Fig. 4.3**.
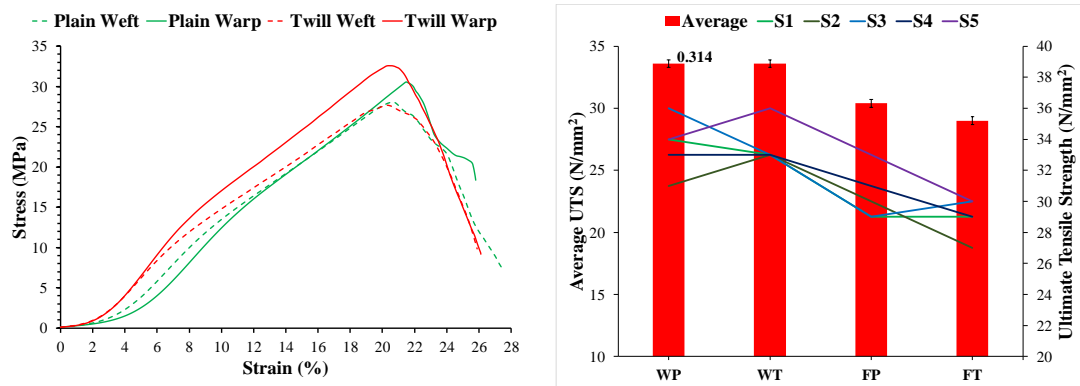
Figure 4. 3: Stress v/s Strain graph of plain weave and twill weave fabric

CHAPTER 5

RESULTS AND DISCUSSION - MECHANICAL TESTING AND FRACTOGRAPHY

In this chapter a detail analysis on the results obtained from the testing such as tensile, flexural and impact carried out to study the bonding between fiber/matrix and failure mechanism of the composites have been discussed.

5.1 Tensile testing

Table 5. 1: Tensile tested results of PWC and TWC

Composites	3P	4P	5P	3T	4T	5T
Ultimate Tensile Strength (MPa)	34.573	34.907	38.681	37.832	37.767	41.320
Strain at UTS (%)	6.480	5.854	5.579	6.195	5.579	7.017
Young's Modulus (GPa)	0.8			0.9		
Stiffness (MN/m)	0.428	0.583	0.733	0.484	0.630	0.793
S.D	1.27	0.79	0.54	1.35	1.52	0.62

A decrease in the slope was observed till 2% strain, due to take up of slack to achieve alignment (**Fig. 5.1**). It was followed by a linear slope, indicating the resistance to the applied load and finally the failure when the load applied was greater than the resistance (Robi et al. 2013). The graph shows sudden failure of composite after reaching the ultimate tensile strength, inferring the brittle nature of material. An increase in strength and stiffness was observed when the thickness increases from 3.1 mm to 5.4 mm. The lowest tensile strength and stiffness were observed for 3.1 mm thickness plain weave i.e. 34.573 MPa and 0.430M N/m and highest for 5.4 mm thickness twill weave composite, 41.320 MPa and 0.793 MN/m respectively. The higher values of strength and stiffness of twill weave composite were attributed to the availability of cellulose observed in XRD graphs (**Fig. 4.2**) and the SEM micrographs (**Fig. 5.6-5.11**) that have shown the presence of resin on the fiber and fiber breakages. Plain weave has low tensile rigidity compared to other weave

forms, thus has resulted in lower values than twill weave composite (Mahmud Zuhudi et al. 2016, Safarabadi and Mohammadi 2018). By hindering the crack propagation and transverse failure of composites, effective load transfer was achieved (Agarwal et al. 2009). Similar results were observed for bamboo mat/epoxy with an increasing thickness (Jena et al. 2013). Twill weave has shown 13% increase in modulus compared to plain weave composite as observed from **Fig. 5.2**.
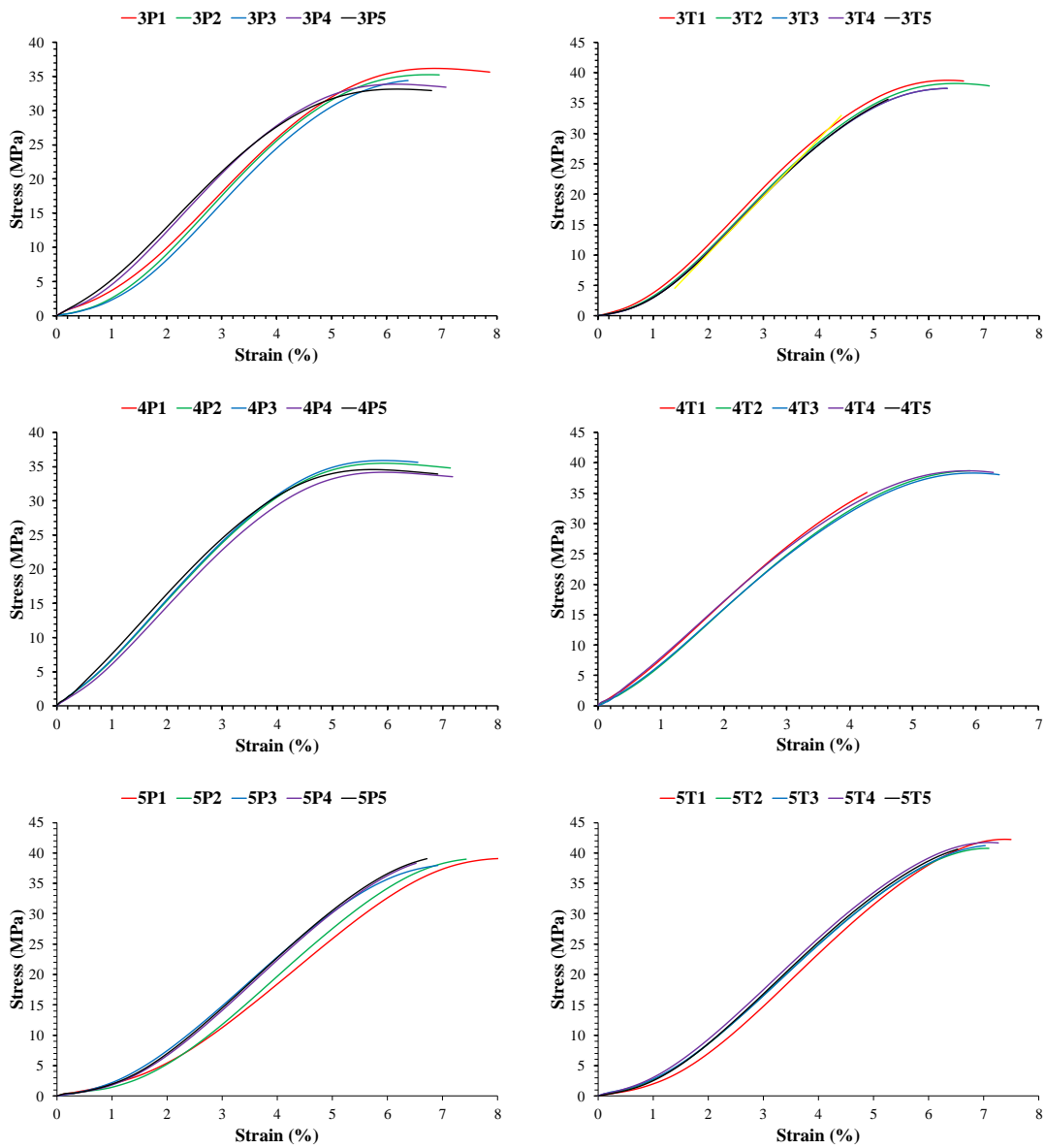
Figure 5. 1: Stress v/s Strain graph of PWC and TWC
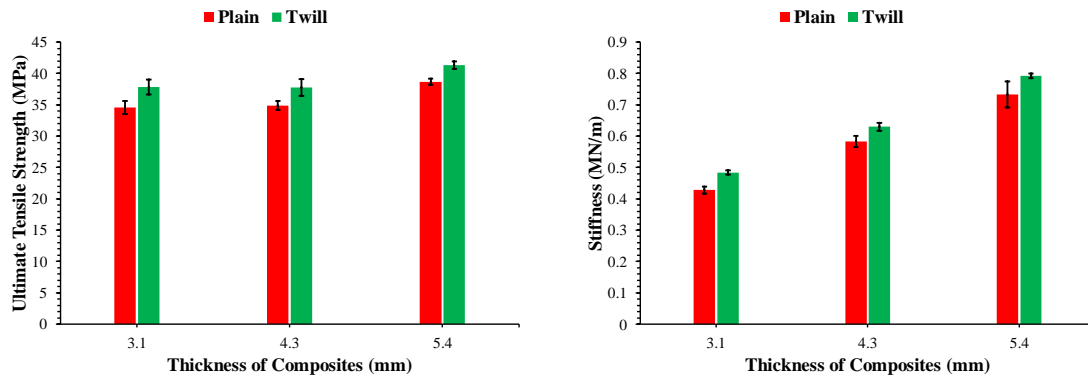
Figure 5. 2: UTS and Stiffness v/s Thickness of PWC and TWC

5.2 Flexural Testing

Table 5. 2: Flexural tested results of PWC and TWC

Composites	3P	4P	5P	3T	4T	5T
Flexural Strength (MPa)	51.897	58.6224	59.457	62.746	62.588	72.245
Flexural Modulus (GPa)	1.9			2.3		
Stiffness (MN/m)	0.219	0.271	0.271	0.292	0.309	0.357

It can be inferred from graphs (**Fig 5.4**) that till 4.3 mm thickness for plain weave composite the values increased and saturated later. For twill weave composite, the values were stable till 4.3 mm thickness and increased later for 5.4 mm thickness. The lowest flexural strength and stiffness observed for 3.1 mm thickness plain weave composite was 51.897 MPa and 0.219 MN/m and highest for 5.4 mm thickness twill weave composite, 72.245 MPa and 0.357 MN/m respectively. It was determined from the graph that under flexural conditions, 5.4 mm thickness twill weave composite has shown an increase of 22% in flexural strength and 28% in stiffness compared to 5.4 mm thickness plain weave composite (**Fig. 5.3**). But flexural strength has shown 1.5 times the ultimate tensile strength values. The higher performance of twill weave composite was attributed to the amount of cellulose determined from XRD graphs **(Fig. 4.2).** The amount of cellulose participated in bonding in twill weave has hindered the crack propagation and by achieving effective load transfer, an increase in strength and stiffness was observed (Jena et al. 2013). Similar trend has been

reported in the literature (Wypych 2016). The flexural modulus of twill weave was 17% higher than that of plain weave composite.
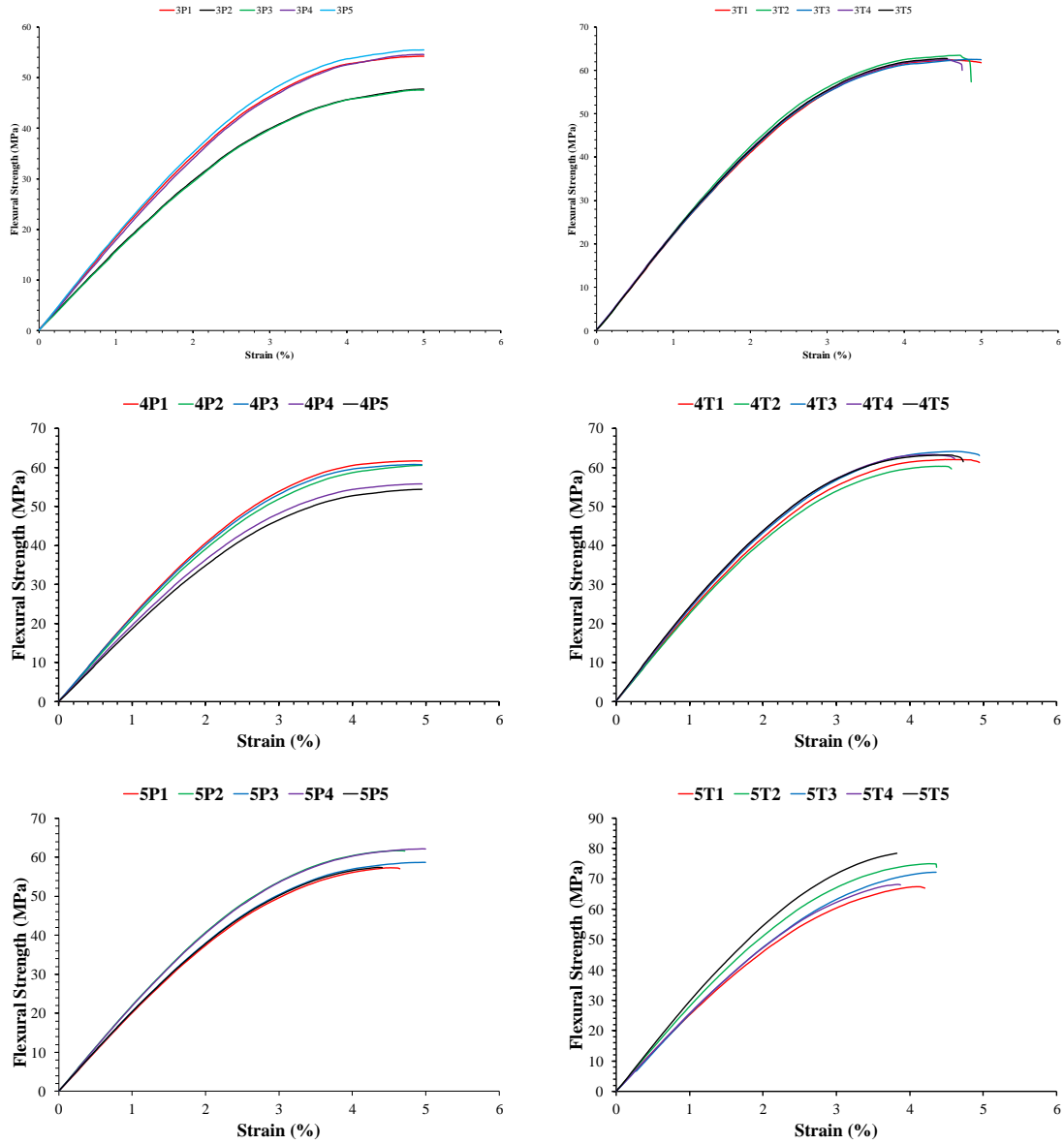
Figure 5. 3: Stress v/s Strain graph of PWC and TWC
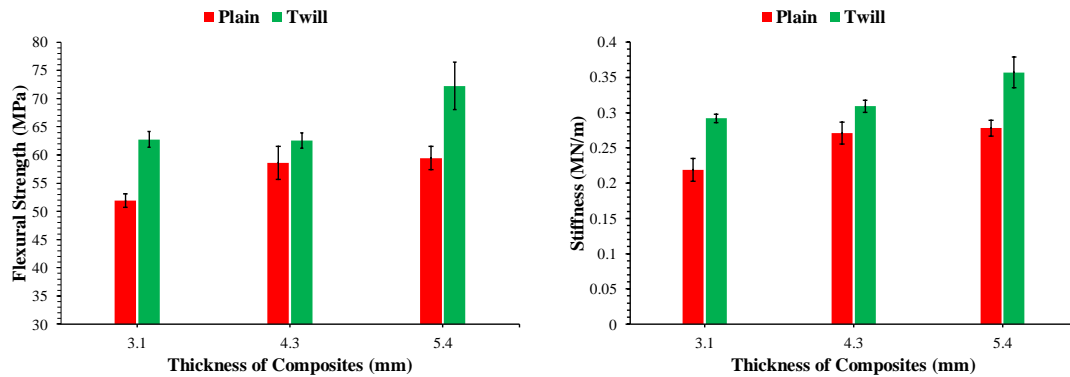
Figure 5. 4: Flexural strength and Stiffness v/s Thickness of PWC and TWC

5.3 Izod Impact Testing

Table 5. 3: Impact tested results of PWC and TWC

Composites	3P	3T	4P	4T	5P	5T
Absorbed energy (J)	0.261	0.316	0.393	0.408	0.316	0.542
Impact Strength (J/m)	84	102	92	95	87	100

Fig. 5.5 shows that the weave pattern and thickness of composite had an effect on impact strength and absorbed energy of plain weave and twill weave composites. During impact, longitudinal and transverse waves generated by the loading have resulted in yarn pullout or breakage at the crossover points and reduced the absorption of maximum energy along the length. Crossover points were more in plain weave than twill weave, thus exhibiting lower strength than twill weave composites (Chen 2016). The variation in the strength was due to the crack propagation under impact condition (Mahmud Zuhudi et al. 2016, Tong et al. 2002, Jena et al. 2013). An increase in the absorbed energy similar to plain woven carbon/epoxy laminates has been observed with an increase in thickness (Xu et al. 2016).
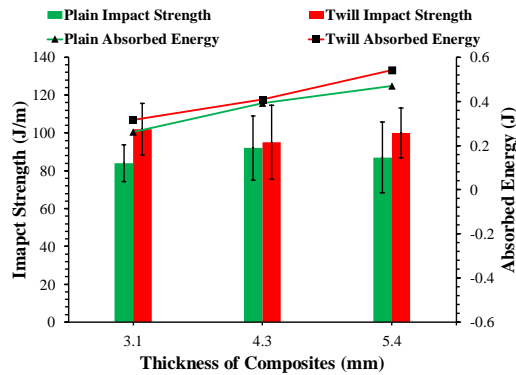
Figure 5. 5: Impact strength v/s Thickness of PWC and TWC

5.4 Fractography of tensile tested specimens

The specimens were cut along the failure and were studied on fractured surface i.e. vertical (V) and the surface perpendicular to the load applied (H). Due to weak bonding of fiber with matrix, fiber imprints were observed for 3.1 mm thickness plain weave composites. High tensile stresses and low shear stresses formed at the interface have resulted in fiber pullout, because of poor bonding (Hyer 1998). Pulled out fibers have displayed very less amount of resin on their surface. Matrix fracture was observed due to inefficient bonding or crack propagation along the weak links (**Fig. 5.6**). 3.1 mm thickness twill weave composites showed fiber breakage and less fiber pullouts along the matrix failure. Matrix cracking observed normal to loading direction indicates brittle nature of the material (Talreja and Varna 2016, Hyer 1998). More areas showed fiber bundle failures. Fiber/matrix de-bonding initiated the fiber pull out that led for failure. The crack propagated through the interface was followed by fiber breakage (**Fig. 5.7**) (Talreja and Varna 2016).
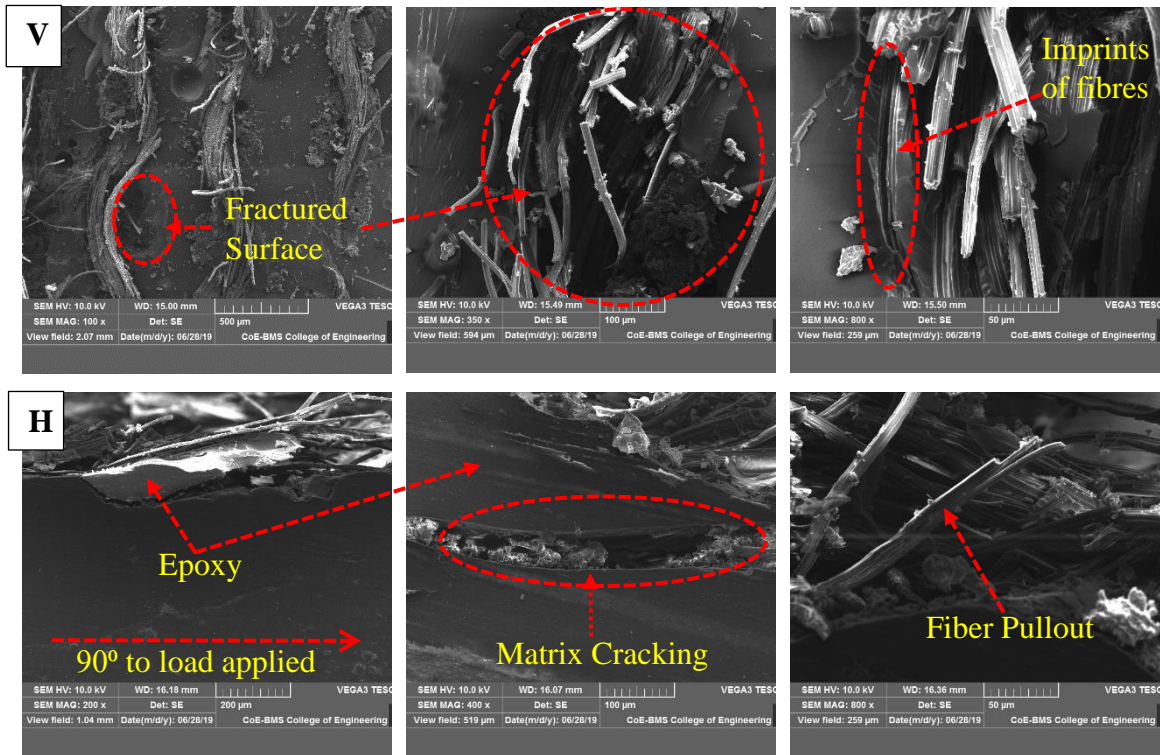
Figure 5. 6: Micrographs of 3.1 mm PWC
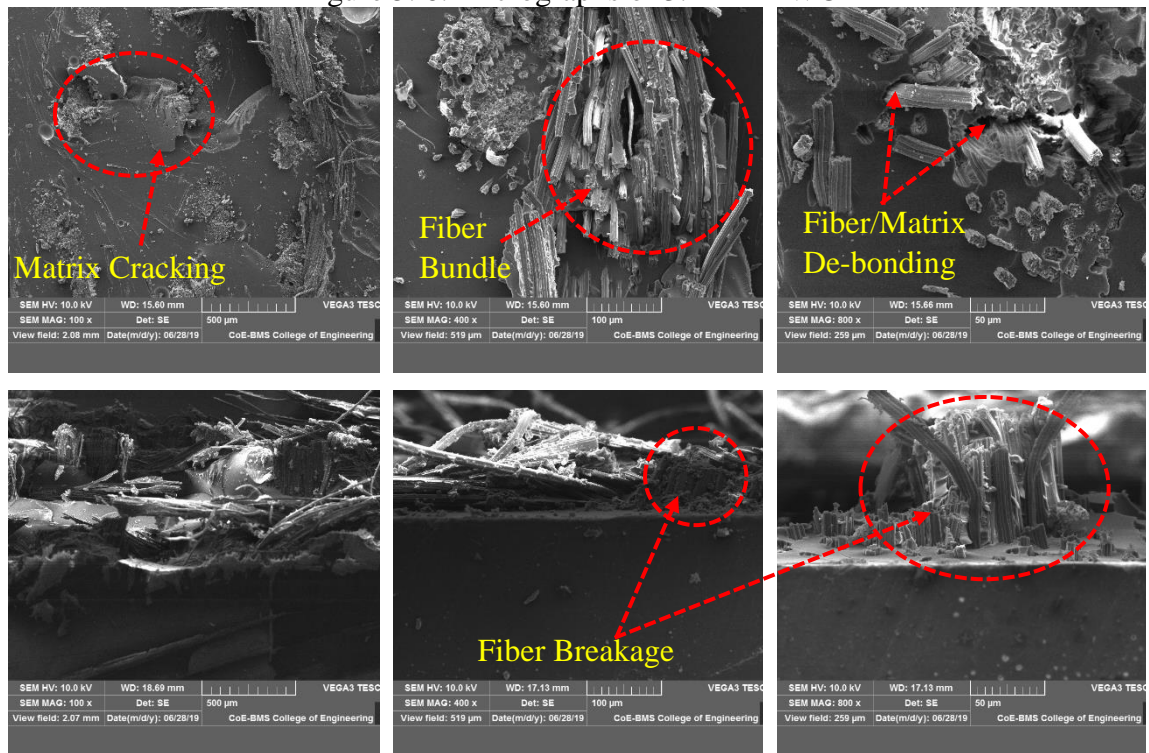
Figure 5. 7: Micrographs of 3.1 mm TWC

An increase in the size of voids, matrix cracking and fiber pullouts were observed for 4.3 mm thickness plain weave composites. Fiber bending was observed only in the plain weave, because the interlacing increases the tendency of bending in yarns (Mahmud Zuhudi et al. 2016). The resin rich areas known as the weakest areas showed the failure around their edges (Hyer 1998) (**Fig. 5.8**). Entrapped gases formed during polymerization, did not play any role in the initiation of crack. Fiber embedded in matrix indicated better wetting for 4.3 mm thickness twill weave composite. Fiber breakage showed no interface failure. The matrix failure took place along the line of loading as shown with few micro-cracks and surface voids (**Fig 5.9**).
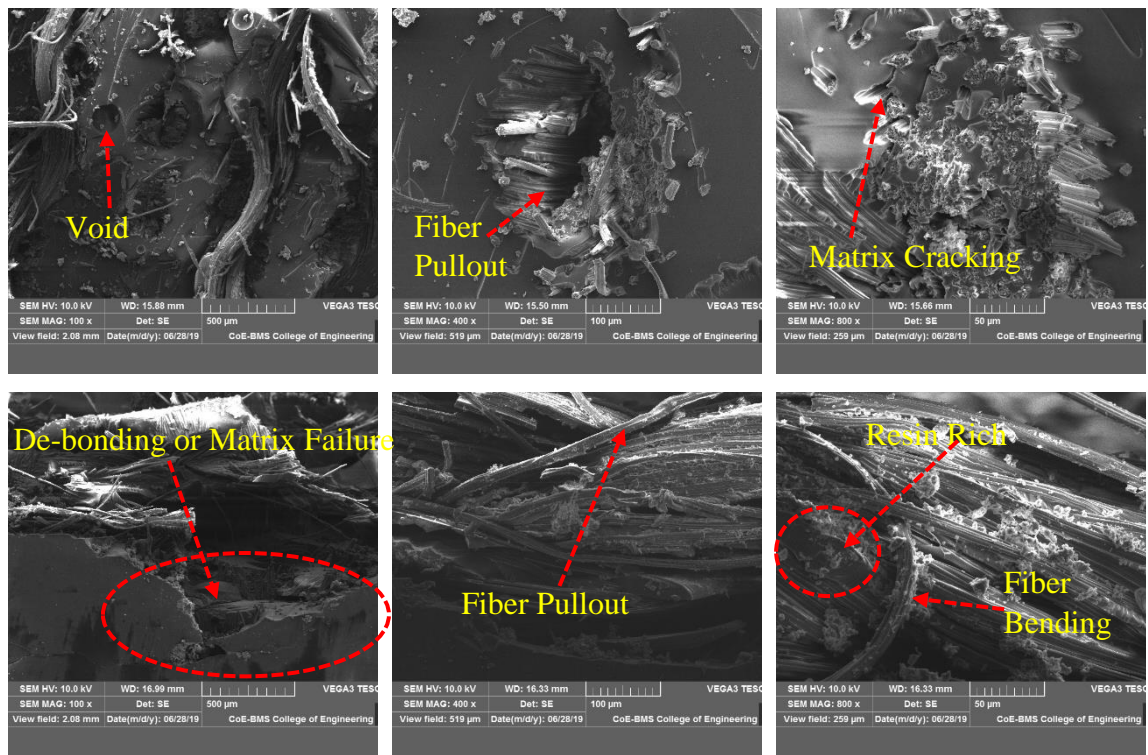
Figure 5. 8: Micrographs of 4.3 mm PWC
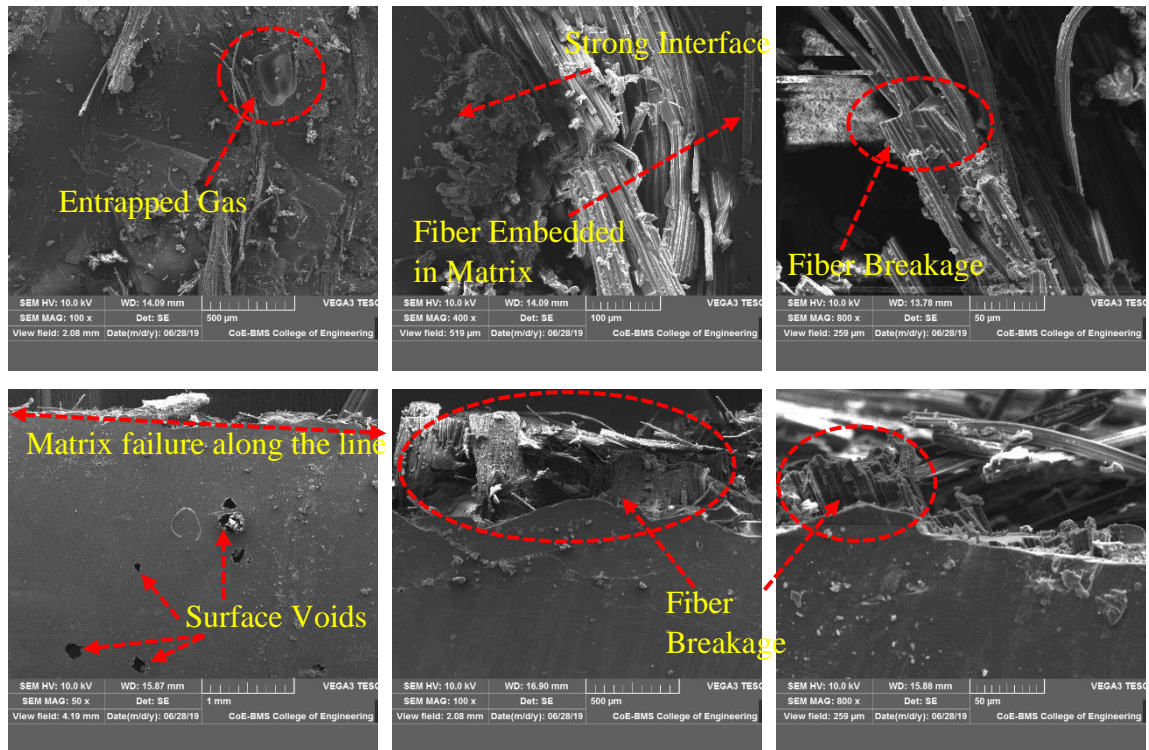
Figure 5. 9: Micrographs of 4.3 mm TWC

With an increase in the thickness, fiber pullouts reduced and fiber breakages were observed for 5.4 mm thickness plain weave composite. The amount of voids and entrapped gases increased with the thickness. Propagation of crack was observed from the edges of voids, indicating they have an effect on the performance (**Fig. 5.10**). Matrix cracking and failure were observed with fiber breakage. Presence of continuous resin on the fibers confirmed better bonding and strong interface. Micro-cracks were observed on the surface near to failure, inferring the load was transferred perpendicular to load applied. Presence of river lines showed the direction of crack propagation in 5.4 mm thickness twill weave composite (**Fig. 5.11**). The SEM images have shown few fiber pullouts, more fiber breakages and presence of resin on the fiber for twill weave composites, thus supporting the results obtained from XRD graphs (Rassiah et al. 2017, Kanaginahal and Murthy 2017).
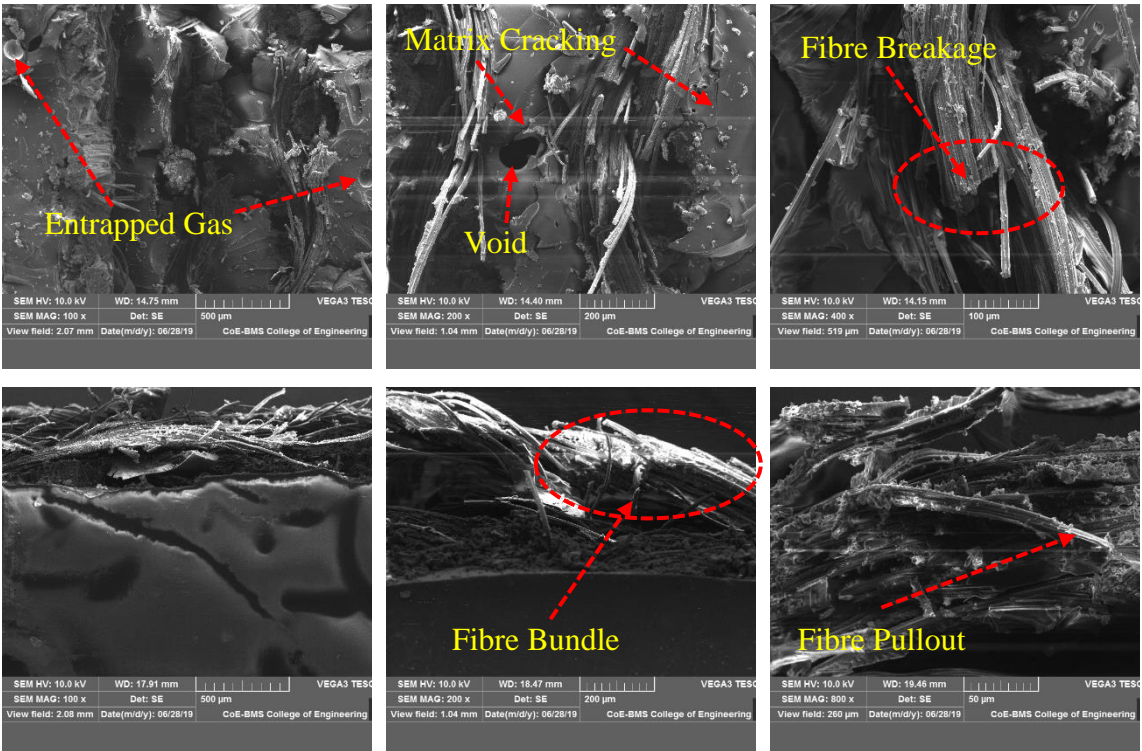
Figure 5. 10: Micrographs of 5.4 mm PWC
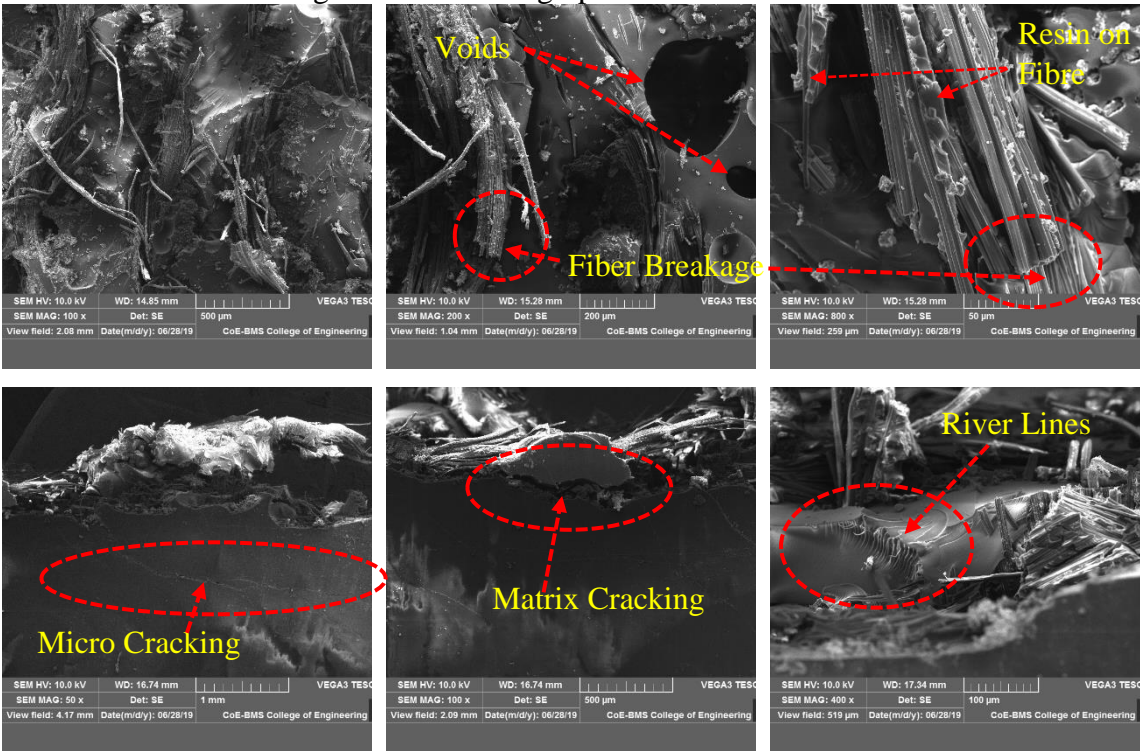
Figure 5. 11: Micrographs of 5.4 mm TWC

CHAPTER 6

RESULTS AND DISCUSSION - THERMAL TESTING AND DYNAMIC MECHANICAL ANALYSIS

In this chapter, a detailed analysis on the results obtained from the testing carried out to study the behaviour of composites under extreme temperatures have been discussed.

6.1 Thermo-Gravimetric Analysis (TGA)

Table 6. 1: TGA results of fabrics, PWC and TWC

Sample	TGA				
	$T_{5\%}$	$T_{20\%}$	$T_{50\%}$	T_{max}	Char @ 650
Plain	46	294	330	332	1.776
Twill	54	301	336	347	1.049
3P	278	329	388	424	10.517
4P	267	327	375	430	10.714
5P	284	340	394	432	10.88
3T	274	329	382	438	11.881
4T	270	328	382	430	11.43
5T	275	330	382	434	11.085

A 3 step degradation was observed from TG curve for fabric. In **Fig. 6.1a,** the 1st degradation before 100 ⁰C implied the presence of water in plain and twill weave fabric. The 2nd degradation with steep loss between 240 ⁰C to 360 ⁰C was due to breaking of hemicellulose and glycosidic linkage of cellulose form a cleavage. At 400 ⁰C the weight loss was due to degradation of lignin, cellulose and finally carbon residue i.e. char at 500 ⁰C (Dorez et al. 2013). In the TG curve, at 5% weight loss the fabrics started to degrade at 50±5 ⁰C and their respective composites degraded at 275 ± 10 ⁰C. Thus the thermal stability of composites increased by **50%** at initial degradation temperature (IDT) compared to their fabrics. The weight loss after 275 ⁰C reduced for PWC and TWC with increasing temperature compared to their fabrics and an increase of **25%** in final

degradation temperature (FDT) was observed (Porras and Maranon 2012, dos Santos et al. 2018, Md Shah et al. s2017). The char residue observed from **Table 6.1** for PWC and TWC was **10 times** more than fabrics, indicating the matrix acted as coating and enhanced the thermal stability of composites.

In DTG curve **Fig. 6.1b**, displays a lower rate of mass loss for PWC and TWC compared to their fabrics respectively, indicating the interface bonding enhanced the thermal stability of fabrics. A larger mass from fabrics gets degraded at 350 ℃, whereas their respective composites sustain till 450 ℃ due to interface bonding and the matrix which protects the reinforcement from degrading (Krishnan 2015, Zhang et al. 2018, Dayo et al. 2017). A peak observed at 440 ℃ was the aliphatic chain present in Manich base of matrix, indicating the presence of cardanol (Pathak and Rao 2006).
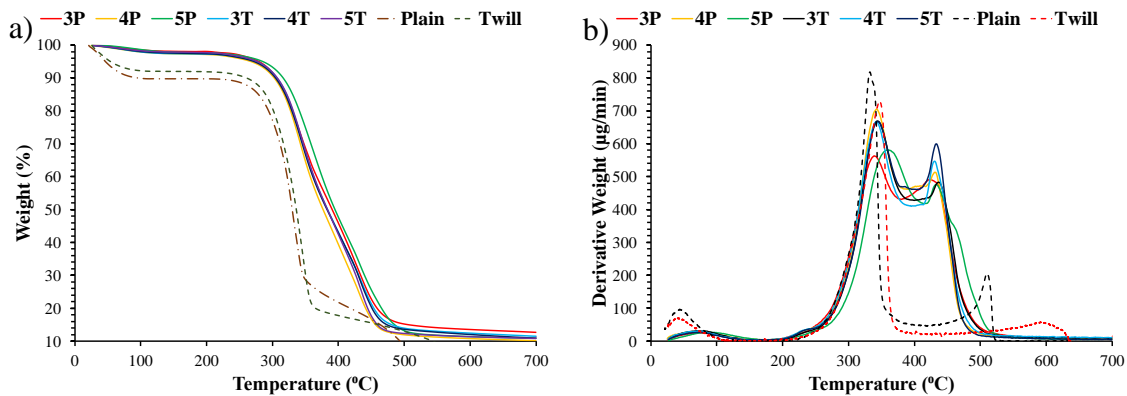
Figure 6. 1: a) TG curve | b) DTG curve of fabrics, PWC and TWC

6.2 Differential Scanning Calorimeter (DSC)

Table 6. 2: DSC results of fabrics, PWC and TWC

Sample	Plain	Twill	3P	4P	5P	3T	4T	5T
T_g	-	-	84.12	83.47	84.28	88.78	87.24	87.72

An endothermic broad curve observed in **Fig 6.2a,** at 125 ℃ indicated presence of moisture and an exothermic peaks at 350 ℃ indicated the breakage of cellulose chains and pyrolysis of lignin, similar results have been observed in DTG curves **Fig 6.1b**. T_g can be determined for semi-crystalline or amorphous structures, for fabrics it was unable to determine

(Amatosa et al. 2019) (Fangueiro and Rana 2016). T_g values observed from **Table 1** was 5% higher for TWC compared to PWC, indicating better bonding and curing for TWC. In **Fig. 6.2b,** the higher peaks observed for 5T inferred better bonding and heat absorption capacity (Naveen et al. 2019) (Wang and Ying 2014). No exothermic peaks were observed below 150 ⁰C/ 200 ⁰C indicating a **faster curing** of PWC and TWC at room temperature (Wang et al. 2019). The exothermic curves observed around 240 ⁰C were due to reaction of side chains of matrix (Kaur and Jayakumari 2016).
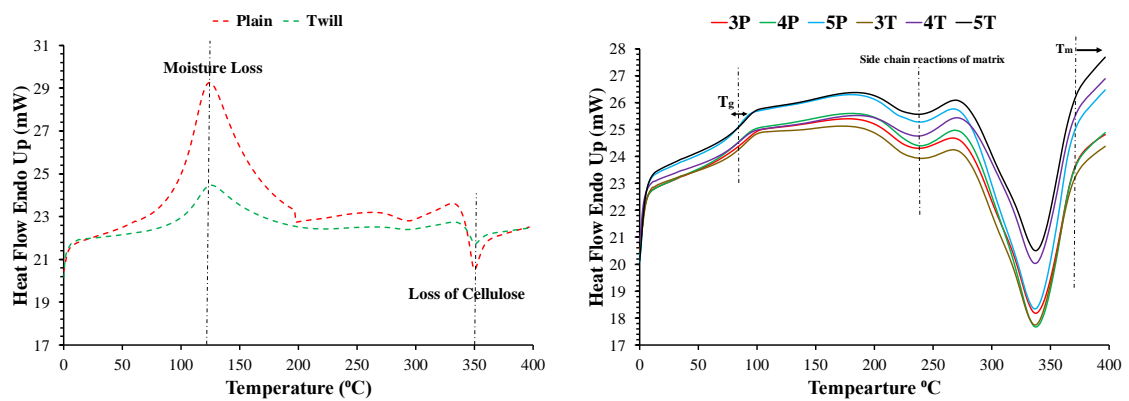
Figure 6. 2: a) First heating of fabrics | b) Second heating of PWC and TWC

6.3 Dynamic Mechanical Analysis (DMA)

6.3.1   Storage Modulus

The molecular mobility in the glassy region (< 60 ⁰C) gets restricted due to strength of intermolecular forces generated by closely packed components, indicating the sample recovery (Ridzuan et al. 2016). In **Fig. 6.3,** 5T displayed a higher E´ inferring better elastic properties in glassy region (Hossain et al. 2011) (Panwar and Pal 2017). It was due to the crystallinity and availability of cellulose observed in XRD for twill weave (Kanaginahal et al. 2019). The stored energy by components breaks loose at the beginning of T_g range as per micro-Brownian motion and with the relaxation of amorphous phase, they co-ordinate large scale motions forming a steep slope in transition region (>60 ⁰C and <100 ⁰C) (Zuhudi et al. 2016). With increasing temperature the matrix softens, thus increasing the free flow of components in rubbery region (>100 ⁰C) (Dayo et al. 2017). In rubbery region the

maximum interface bonding or interfacial strength was determined from crosslinking density equation $\rho = E' / (\Phi RT)$ where ρ is crosslink density, Φ is front factor normalized to 1, R is gas constant and T is absolute temperature i.e. $T_g + 30$ ºC (Zhang and Xu 2019). The ρ calculated displayed in **Table 6.3**, from the rubbery region was higher for TWC than PWC in order of 3T>5T>4T>5P>3P>4P. The E′ of 5T showed **1.3 times** that of 5P in rubbery region, indicating better stiffness (Espinach et al. 2018).

Table 6. 3: Crosslink density of PWC and TWC in rubbery region

Crosslink	3P	4P	5P	3T	4T	5T
density	0.0533	0.0574	0.0601	0.0817	0.0752	0.0793
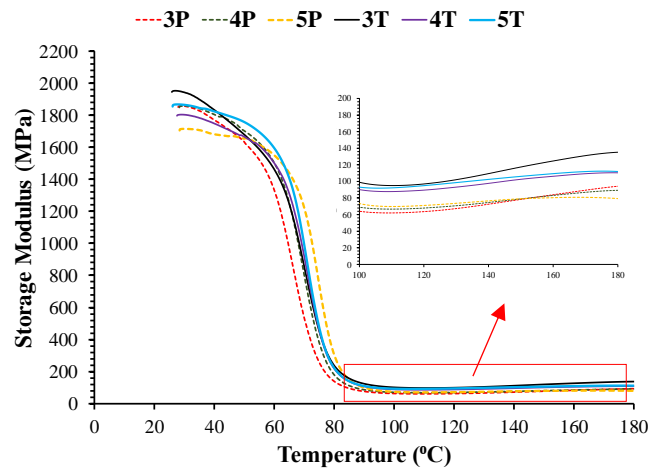
Figure 6. 3: Storage modulus v/s Temperature of PWC and TWC

6.3.2 Loss Modulus

E′′ of a material will be measured based on load, temperature, geometry and displacement. An unrecoverable energy dissipated in form of heat due to segmental motion of components at interface results in E′′. A higher cross-linking density of TWC have restricted the polymer chain motion compared to PWC displaying lower values in **Fig**. **6.4**, (Sreenivasan et al. 2015). The ratio of bonding sites to thickness was higher for TWC (Kanaginahal et al. 2019), compared to PWC. 5T showed 9% higher E′′ and a higher T_g, indicating better bonding at interface (Song et al. 2012). A higher loss modulus displayed

by 5T indicates dissipation of high energy due to internal friction or molecular motion at interface (Kumar and Das 2017). The T_g values obtained here show the realistic values of the transitions happening at the interface of composites than the loss factor values (Jawaid et al. 2012). The area under the curve for both the composites have been same, indicating the volume fraction of reinforcement maintained was constant.
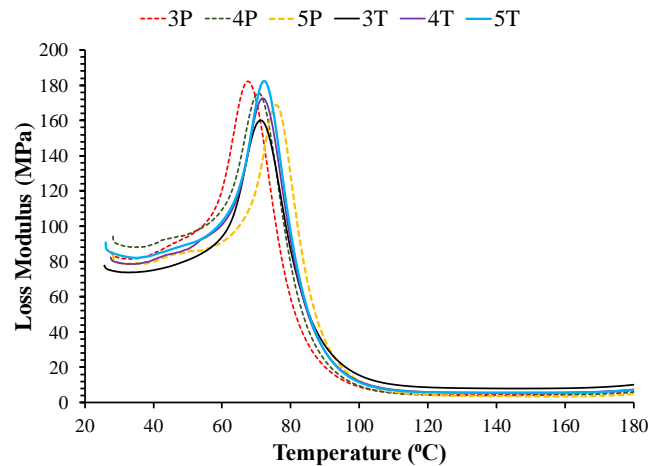
Figure 6. 4: Loss modulus v/s Temperature of PWC and TWC

6.3.3 Loss Factor (Tanδ)

A lower value of loss factor indicates elastic behaviour and a higher value, damping (Kumar et al. 2011). In **Fig. 6.5**, the number of interlacements were higher for plain weave, thus PWC shows larger peak value. The damping factor has not changed for PWC inferring the stiffer properties of plain weave fabric and distinct interface. A soft fiber-matrix interface has kept the loss factor value of PWC higher indicating its damping behaviour (Fiore and Calabrese 2019). Twill weave pattern has a higher float length with less interlacements, thus with increasing thickness the tanδ peak increased (Rouf et al. 2017) (Rajesh et al. 2018). The T_g values of TWC showed no change whereas for PWC the value increased by 2.5% with increasing thickness. 5T has shown a higher value of storage and loss modulus than PWC indicating a better damping property in glassy and rubbery regions (Song et al. 2012).
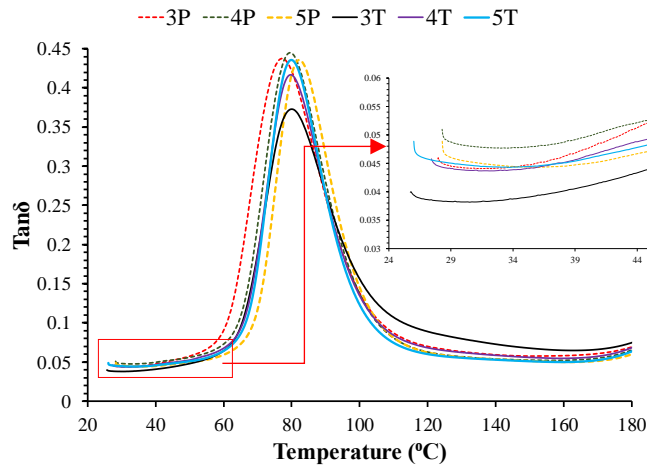
Figure 6. 5: Loss factor v/s Temperature of PWC and TWC

6.3.4 Cole-Cole plot

In **Fig. 6.6**, PWC have shown an elliptical shape indicating a multiphase formation at the interphase, whereas TWC displayed a semi-circle inferring a homogenous formation (Panwar and Pal 2017). With increasing thickness the peaks of TWC increased and were higher for 5T, whereas it reduced for PWC. The overall results infer thickness and weave pattern of composites have an influence on visco-elastic behavior and TWC has shown better damping properties.
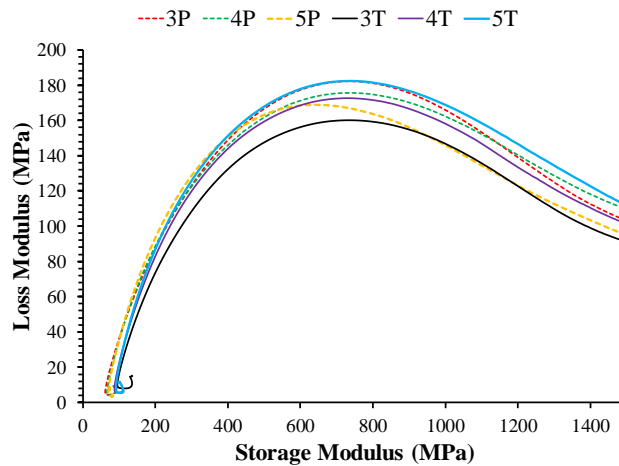
Figure 6. 6: Cole-Cole plot of PWC and TWC

CHAPTER 7

RESULTS AND DISCUSSION - WATER ABSORPTION AND FLAMMABILITY

In this chapter, a detailed analysis on the results obtained from the testing carried out to study the water absorption behaviour and sustainability to flammability conditions have been discussed.

7.1 Water Absorption

Table 7. 1: Percentage of Water absorption of PWC and TWC of varying thickness

Composite Hours | Solution		3P	4P	5P	3T	4T	5T
2	D	0.24	0.22	0.16	0.21	0.14	0.13
	S	0.18	0.16	0.13	0.14	0.12	0.13
6	D	0.40	0.34	0.29	0.35	0.29	0.26
	S	0.33	0.28	0.24	0.29	0.24	0.23
12	D	0.65	0.55	0.45	0.57	0.45	0.41
	S	0.60	0.47	0.36	0.47	0.38	0.38
24	D	1.04	0.87	0.69	0.88	0.68	0.64
	S	0.97	0.74	0.58	0.71	0.60	0.57
48	D	1.57	1.31	1.04	1.25	1.00	0.95
	S	1.43	1.15	0.89	1.14	0.92	0.89
72	D	2.16	1.76	1.40	1.81	1.47	1.35
	S	2.00	1.58	1.23	1.57	1.29	1.22
96	D	2.81	2.29	1.82	2.36	1.92	1.77
	S	2.62	2.07	1.60	2.06	1.69	1.60
120	D	3.47	2.82	2.25	2.91	2.38	2.18

	S	3.25	2.56	1.98	2.55	2.09	1.98
144	D	4.13	3.35	2.67	3.46	2.84	2.60
	S	3.87	3.05	2.36	3.04	2.49	2.35

The results plotted in graphs the notations stands as 'S'- salt water and 'D'-distilled water. The salt water was collected from Arabian Sea. The specimens immersed in both solutions for one week as the approach was to determine the effect of weave pattern and thickness in hindering water absorption. Water diffusion happens through the micro-gaps between polymer chains, the micro-cracks formed during processing and after swelling and finally through the gaps and flaws at the interphase by capillary action (Väisänen et al. 2017). The water also has affinity towards the amorphous region through which it rushes the water into micro-capillary units known as micro-fibrils. The hydroxyl groups in composites develop new hydrogen bonding with water molecules as water starts to infuse through the cracks, which leads to swelling (Chandrasekaran et al. 2017). With increasing thickness few works have shown an increase in water absorption (Muktha & Keerthi Gowda 2017, Kejariwal & Keerthi Gowda 2017) whereas PWC and TWC in **Fig 7.1,** have shown reduction with increasing thickness due to better interface and availability of crystallinity as observed in XRD (Azwa et al. 2013). The higher percentage of cellulose involved in bonding, better wettability as confirmed by SEM micrographs (Kanaginahal et al. 2019) and the homogenous formation in Cole-Cole plot infer the minimal absorption for TWC compared to PWC. The crossover points in plain weave fabrics were higher than twill weave, thus in PWC the micro-cracks formed at these points were higher and led to more amount of water absorption by capillary action than TWC (Azwa et al. 2013). From **Fig. 7.1a, 7.1b**, increasing thickness has an effect on reducing the water absorption as seen in the graphs under both solutions. With increasing thickness of PWC at 5.4 mm a 34% reduction in water absorption was observed compared to 3.1 mm thickness in D-solution and 37% in S-solution after a week. Similarly TWC showed 23% reduction in D-solution and 20% in S-solution. At 5.4 mm thickness PWC and TWC have shown similar resistance to absorption in both the solutions, whereas TWC has shown a higher resistance at 3.4 mm

and 4.3 mm thickness. In **Fig 7.1**, varying behavior turned into a linear rate of absorption after 4 days, a typical Fickian diffusion behavior in initial periods till attaining saturation (Cuinat-Guerraz et al. 2016). In **Fig. 7.1c, 7.1d**, we can observe the absorption of distilled water was higher compared to salt, it was due to the presence of salt content that hindered the absorption in both the composites (Jena et al. 2014).
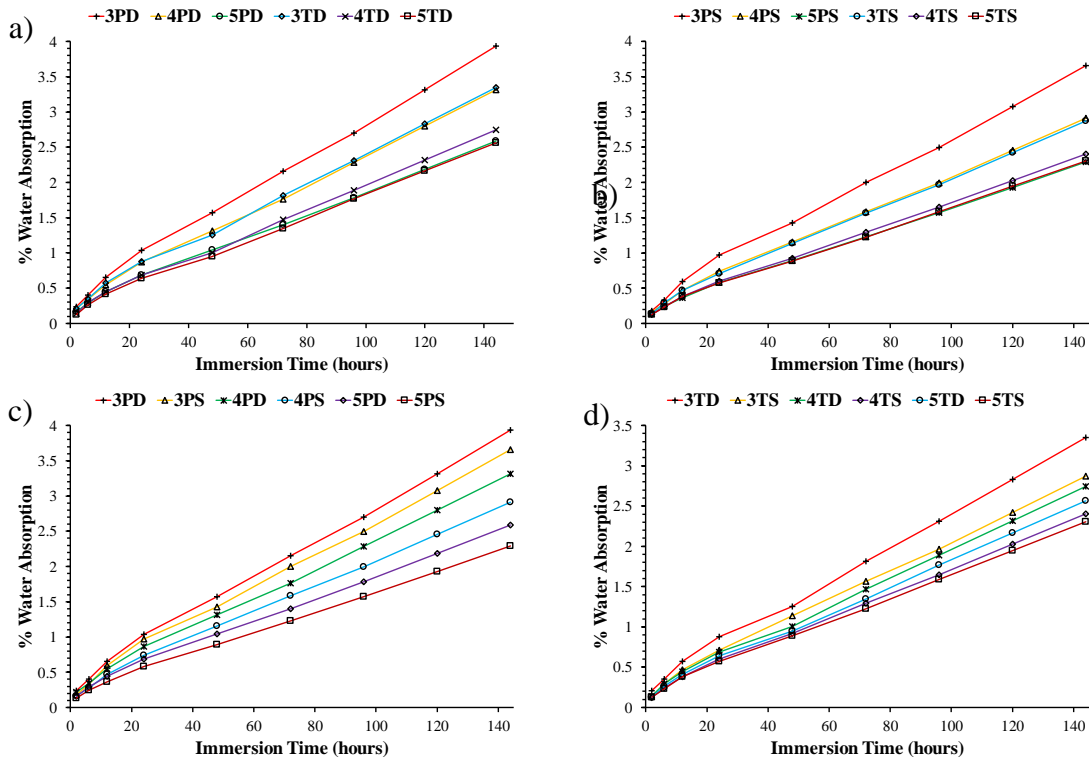
Figure 7. 1: a) Distilled water | b) Salt water| c) PWC | d) TWC

7.2 Flammability

Table 7. 2: Horizontal burning results of PWC and TWC of varying thickness

Sample	Seconds to burn damaged length	Burning rate (mm/min)	HB
3P1	214.96	21.08	Pass
4P1	202.73	22.28	Pass
5P1	278.63	16.13	Pass
3T1	204.7	22.01	Pass

| 4T1 | 207.73 | 21.73 | Pass |
| 5T1 | 277.43 | 16.56 | Pass |

The graph has been plotted in **Fig 7.2**, shows weave pattern has minimal impact on the flammability of composites. It can be deduced from graph, that with an increase in thickness, increased the time for ignition by reducing the burning rate (Fateh et al. 2017). The burning rate has not shown much of change from 3.1 mm to 4.3 mm thickness, but for 5.4 mm thickness a 30% decrease in the burning rate was observed. Flame propagation was reduced due to wettability of composites (Salim et al. 2018) observed in SEM micrographs for 5.4 mm thickness (Kanaginahal et.al 2019).
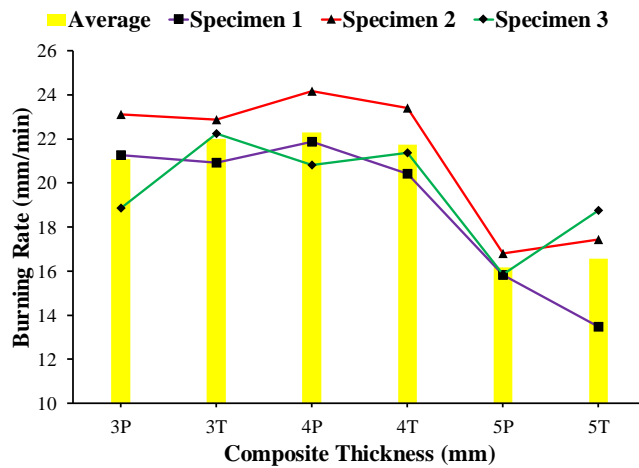
Figure 7. 2: Horizontal burning rate v/s Thickness of PWC and TWC

CHAPTER 8

CONCLUSIONS

1. FTIR analysis indicated the presence of cellulose and polysaccharides in bamboo fiber, presence of cardanol in matrix and bonding of reinforcement with matrix

2. XRD analysis showed higher intensity peaks for twill weave, inferring more amount of cellulose available for bonding

3. The tensile strength of twill weave fabric was found to be 7% higher than that of the plain weave fabric

4. Tensile results showed higher values of strength and stiffness for twill weave composites with an increase in thickness

5. Twill weave composites with 5.4 mm thickness showed an increase of 12% in tensile strength and 8% increase in stiffness compared to 5.4 mm thickness plain weave composite

6. Flexural results showed higher values of strength and stiffness with an increase in the thickness of composite for twill weave composite

7. Twill weave composite with 5.4mmthickness showed an increase of 22% in flexural strength and 28% in stiffness compared to 5.4mmthickness plain weave composite

8. Izod impact results displayed an increase of 16% in absorbed energy for 5.4mmthickness twill weave composite when compared with 5.4 mm thickness plain weave composite

9. Fractured specimens of tensile test showed fiber pullouts for plain weave and fiber breakages for twill weave composites

10. TGA of composites showed a 50% improvement in IDT and 25% enhancement in FDT as compared to their respective fabrics. The weave pattern and thickness of composite had minimal impact on degradation of composites

11. Char residue of PWC and TWC showed 10 times improvement in thermal stability compared to their fabrics

12. DSC analysis showed a 5% higher value of T_g for WC compared to PWC. A faster curing rate was noticed for PWC and TWC at room temperature. T_m of PWC and TWC was notified at 370 ⁰C with 5T displaying better heat absorbing capacity

13. DMA showed 1.3 times higher storage and 9% higher loss modulus along with homogenous curve for 5T compared to 5P, indicating better damping properties. 5T displayed higher value of homogenous interface

14. TWC have shown better resistance to absorption, 3T showed an improvement of 21.4% and 4T showed 18.4% in resisting the absorption compared to 3P and 4P, respectively. 5P and 5T have shown similar resistance to water absorption, due to their better wettability

15. Better wettability and composite thickness influenced the flame resistant of composites, whereas weave pattern had negligible effect. 5.4 mm thickness of PWC and TWC reduced the burning rate by 30% compared to 3.1 mm thickness respectively

References

Abdul Khalil, H. P. S., Che Mohamad, H. C. I., Khairunnisa, A. R., Owolabi, F. A. T., Asniza, M., Rizal, S., Fazita, M. R. N., and Paridah, M. T. (2018). "Development and Characterization of Bamboo Fiber Reinforced Biopolymer Films." *Mater. Res. Express*, 5(8), 1–10.

Alantali, A., Alia, R. A., Umer, R., and Cantwell, W. J. (2018). "Scaling Effects in the Manufacture and Testing of Grid-Stiffened Composite Structures." *J. Compos. Mater.*, 52(17), 2351–2363.

Alavudeen, A., Rajini, N., Karthikeyan, S., Thiruchitrambalam, M., and Venkateshwaren, N. (2015). "Mechanical Properties of Banana/Kenaf Fiber-Reinforced Hybrid Polyester Composites: Effect of Woven Fabric and Random Orientation." *Mater. Des.*, 66, 246–257.

Amatosa, T. A., Loretero, M. E., Manilhig, M. G., Laksono, A. D., and Yen, Y.-W. (2019). "Determination of Thermal Properties and Fire Retardant Ability of Philippine Bamboo as Natural Thermal Insulation." *Int. J. Appl. Eng. Res.*, 14(8), 1764–1771.

Arrakhiz, F. Z., Malha, M., Bouhfid, R., Benmoussa, K., and Qaiss, A. (2013). "Tensile, flexural and torsional properties of chemically treated alfa, coir and bagasse reinforced polypropylene." *Compos. Part B Eng.*, 47, 35–41.

Azeez, M. A., and Orege, J. I. (2013). "Bamboo, Its chemical modification and products." *Bamboo - Curr. Futur. Prospect.*, INTECHOPEN LIMITED No. 11086078 Registered Office: 5 Princes Gate Court, London, SW7 2QJ, UK, 25–40.

Azwa, Z. N., Yousif, B. F., Manalo, A. C., and Karunasena, W. (2013). "A Review on The Degradability of Polymeric Composites Based on Natural Fibres." *Mater. Des.*, 47, 424–442.

Balaji, A., Karthikeyan, B., Swaminathan, J., and Sundar Raj, C. (2017). "Mechanical Behavior of Short Bagasse Fiber Reinforced Cardanol-Formaldehyde Composites."

Fibers Polym., 18(6), 1193–1199.

Banga, H., Singh, V. K., and Choudhary, S. K. (2015). "Fabrication and Study of Mechanical Properties of Bamboo Fibre Reinforced Bio-Composites." *Innov. Syst. Des. Eng.*, 6(1), 84–98.

Barreto, A. C. H., Rosa, D. S., Fechine, P. B. A., and Mazzetto, S. E. (2011). "Properties of sisal fibers treated by alkali solution and their application into cardanol-based biocomposites." *Compos. Part A Appl. Sci. Manuf.*, 42(5), 492–500.

Benega, M. A. G., Raja, R., and Blake, J. I. R. (2017). "A preliminary evaluation of bio-based epoxy resin hardeners for maritime application." *Procedia Eng.*, 200, 186–192.

Biswas, S., Ahsan, Q., Cenna, A., Hasan, M., and Hassan, A. (2013). "Physical and Mechanical Properties of Jute, Bamboo and Coir Natural Fiber." *Fibers Polym.*, 14(10), 1762–1767.

Biswas, S., Shahinur, S., Hasan, M., and Ahsan, Q. (2015). "Physical, Mechanical and Thermal Properties of Jute and Bamboo Fiber Reinforced Unidirectional Epoxy Composites." *Procedia Eng.*, 105, 933–939.

Caldas, A., Santos, J. C. dos, Panzera, T. H., and Strecker, K. (2016). "Mechanical properties of epoxy banana fibre composite treated with sodium carbonate." *BCCM3-Brazilian Conf. Compos. Mater.*, Brazil, 1–6.

Campbell, F. C. (2010). *Structural Composite Materials*. ASM International, Materials Park, OH 44073-0002.

Chandrasekaran, M., Ishak, M. R., Sapuan, S. M., Leman, Z., and Jawaid, M. (2017). "A Review on The Characterisation of Natural Fibers and Their Composites After Alkali Treatment and Water Absorption." *Plast. Rubber Compos.*, 46(3), 119–136.

Chen, X. (2016). "Ballaistic damaeg of hybrid composite materials Thermoplastic matrix combat helmet with carbon-epoxy skin for ballistic performance." Woodhead Publishing, 115, 444.

Costa Júnior, A., Barreto, A., Rosa, D., Maia, F., Lomonaco, D., and Mazzetto, S. (2015). "Thermal and Mechanical Properties of Biocomposites Based on a Cashew Nut Shell Liquid Matrix Reinforced With Bamboo Fibers." *J. Compos. Mater.*, 49(18), 2203–2215.

Cuinat-Guerraz, N., Dumont, M.-J., and Hubert, P. (2016). "Environmental Resistance of Flax/Bio-Based Epoxy and Flax/Polyurethane Composites Manufactured by Resin Transfer Moulding." *Compos. Part A Appl. Sci. Manuf.*, 88, 140–147.

Dash, D., Samanta, S., Gautam, S. S., and Murlidhar, M. (2013). "Mechanical Characterizations of Natural Fiber Reinforced Composite Materials." *Int. J. Adv. Mater. Manuf. Charact.*, 3(5), 1–6.

Dayo, A. Q., Gao, B., Wang, J., Liu, W., Derradji, M., Shah, A. H., and Babar, A. A. (2017). "Natural Hemp Fiber Reinforced Polybenzoxazine Composites: Curing Behavior, Mechanical and Thermal Properties." *Compos. Sci. Technol.*, 144, 114–124.

Deepak, P., Vignesh Kumar, R., Badrinarayanan, S., Sivaraman, H., and Vimal, R. (2017). "Effects of Polyamide and/or Phenalkamine Curing Agents on the Jute Fibre Reinforcement with Epoxy Resin Matrix." *Mater. Today Proc.*, 4(2), 2841–2850.

Dhakal, S., and Keerthi Gowda, B. S. (2017). "An Experimental Study on Mechanical properties of Banana Polyester Composite." *Mater. Today Proc.*, 4(8), 7592–7598.

Dhanalakshmi, S., Ramadevi, P., and Basavaraju, B. (2015). "Influence of Chemical Treatments on Flexural Strength of Areca Fiber Reinforced Epoxy Composites." *Chem. Sci. Trans.*, 4(2), 409–418.

Dong, Y., Ghataura, A., Takagi, H., Haroosh, H. J., Nakagaito, A. N., and Lau, K.-T. (2014). "Polylactic acid (PLA) biocomposites reinforced with coir Fibres: Evaluation of mechanical performance and multifunctional properties." *Compos. Part A Appl. Sci. Manuf.*, 63, 76–84.

Dorez, G., Taguet, A., Ferry, L., and Lopez-Cuesta, J. M. (2013). "Thermal and Fire Behavior of Natural Fibers/PBS Biocomposites." *Polym. Degrad. Stab.*, 98(1), 87–95.

Espinach, F. X., Boufi, S., Delgado-Aguilar, M., Julián, F., Mutjé, P., and Méndez, J. A. (2018). "Composites from Poly(lactic acid) and Bleached Chemical Fibres: Thermal Properties." *Compos. Part B Eng.*, 134, 169–176.

Essabir, H., Bensalah, M. O. O., Rodrigue, D., Bouhfid, R., and Qaiss, A. (2016). "Structural, mechanical and thermal properties of bio-based hybrid composites from waste coir residues: Fibers and shell particles." *Mech. Mater.*, 93, 134–144.

Fan, M., and Fu, F. (2016). *Advanced High Strength Natural Fibre Composites in Construction*. *Woodhead Publ.*, Woodhead Publishing Series in Composites Science and Engineering.

Fangueiro, R., and Rana, S. (2016). *Natural Fibres: Advances in Science and Technology Towards Industrial Applications*.

Fateh, T., Kahanji, C., Joseph, P., and Rogaume, T. (2017). "A Study of The Effect of Thickness on The Thermal Degradation and Flammability Characteristics of Some Composite Materials Using a Cone Calorimeter." *J. Fire Sci.*, 35(6), 547–564.

Ferdous, N., Rahman, S., Kabir, R. Bin, and Ahmed, A. E. (2014). "A Comparative Study on Tensile Strength of Different Weave Structures." *Int. J. Sci. Res. Eng. Technol.*, 3(9), 1307–1313.

Fiore, V., and Calabrese, L. (2019). "Effect of Stacking Sequence and Sodium Bicarbonate Treatment on Quasi-Static and Dynamic Mechanical Properties of Flax/Jute Epoxy-Based Composites." *Materials (Basel).*, 12(9), 1–18.

Fiore, V., Scalici, T., Nicoletti, F., Vitale, G., Prestipino, M., and Valenza, A. (2016). "A new eco-friendly chemical treatment of natural fibres: Effect of sodium bicarbonate on properties of sisal fibre and its epoxy composites." *Compos. Part B Eng.*, 85, 150–160.

Francucci, G., Rodríguez, E. S., and Vázquez, A. (2010). "Study of saturated and unsaturated permeability in natural fiber fabrics." *Compos. Part A Appl. Sci. Manuf.*, 41(1), 16–21.

Fuentes, C. A., Brughmans, G., Tran, L. Q. N., Dupont-Gillain, C., Verpoest, I., and Vuure, A. W. Van. (2015). "Mechanical behaviour and practical adhesion at a bamboo composite interface : Physical adhesion and mechanical interlocking." *Compos. Sci. Technol.*, 109, 40–47.

Ghaedi, H., Ayoub, M., Sufian, S., Lal, B., and Uemura, Y. (2017). "Thermal Stability and FT-IR Analysis of Phosphonium-Based Deep Eutectic Solvents with Different Hydrogen Bond Donors." *J. Mol. Liq.*, 242, 395–403.

Hanamanagouda, Gowda, K., G L, E. P., and R, V. (2016). "Mechanical Properties of Raw Jute Polyester Composite." *Int. J. Fiber Text. Res.*, 6(1), 20–24.

Hartoni, J. F., Anshari, B., and Catur, A. D. (2017). "Effect of Core and Skin Thicknesses of Bamboo Sandwich Composite on Bending Strength." *Int. J. Mech. Eng. Technol.*, 8(12), 551–560.

Hossain, M. K., Dewan, M. W., Hosur, M., and Jeelani, S. (2011). "Mechanical Performances of Surface Modified Jute Fiber Reinforced Biopol Nanophased Green Composites." *Compos. Part B Eng.*, 42(6), 1701–1707.

Hyer, M. W. (1998). *Stress Analysis of Fiber-Reinforced Composite Materials*. Singapore: McGraw-Hill Companies.

Indira, K. N., Grohens, Y., Baley, C., Thomas, S., Joseph, K., and Pothen, L. A. (2011). "Adhesion and Wettability Characteristics of Chemically Modified Banana Fibre for Composite Manufacturing." *J. Adhes. Sci. Technol.*, 25, 1515–1538.

Indira, K. N., Parameswaranpillai, J., and Thomas, S. (2013). "Mechanical Properties and Failure Topography of Banana Fiber PF Macrocomposites Fabricated by RTM and CM Techniques." *ISRN Polym. Sci.*, 8, 1–8.

Jawaid, M., Abdul Khalil, H. P. S., and Alattas, O. S. (2012). "Woven Hybrid Biocomposites: Dynamic Mechanical and Thermal Properties." *Compos. Part A Appl. Sci. Manuf.*, 43(2), 288–293.

Jena, H., Pandit, M. K., and Pradhan, A. K. (2013). "Effect of Cenosphere on Mechanical Properties of Bamboo-Epoxy Composites." *J. Reinf. Plast. Compos.*, 32(11), 794–801.

Jena, H., Pradhan, A. K., and Pandit, M. K. (2014). "Studies on Water Absorption Behaviour of Bamboo-Epoxy Composite Filled with Cenosphere." *J. Reinf. Plast. Compos.*, 33(11), 1059–1068.

Joy, Y. J., Retna, A. M., and Samuel, R. K. (2015). "Synthesis and Characterization of Natural Fibre Reinforced Polyurethane Composites Based on Cardanol." *Green Chem. Technol. Lett.*, 1(1), 42–47.

Kalusuraman, G., Siva, I., Jappes, J. T. W., and Campos Amico, S. (2017). "Effect of starch treatment and hybridisation on the mechanical properties of natural fibre composites." *Int . J . Comput. Aided Eng. Technol.*, 9(2), 261–269.

Kanaginahal, G. M., and Murthy, M. (2017). "Microstructural Study and Evaluation of Few Mechanical Properties of Hybrid Composites." *Adv. Mater. Manuf. Charact.*, 7(1), 7–14.

Kanaginahal, G. M., Suresh Hebbar, H., and Kulkarni, S. M. (2019). "Influence of Weave Pattern and Composite Thickness on Mechanical Properties of Bamboo/Epoxy composites." *Mater. Res. Express*, 6(12), 1–13.

Kaur, M., and Jayakumari, L. S. (2016). "Eco-friendly Cardanol-Based Phenalkamine Cured Epoxy-Cenosphere Syntactic Foams: Fabrication and Characterisation." *J. Appl. Polym. Sci.*, 133(46), 1–10.

Kejariwal, R. K., and Keerthi Gowda, B. S. (2017). "Flammability and Moisture Absorption Behavior of Sisal-Polyester Composites." *Mater. Today Proc.*, 4(8), 8040–8044.

Khan, M. A., Guru, S., Padmakaran, P., Mishra, D., Mudgal, M., and Dhakad, S. (2011). "Characterisation Studies and Impact of Chemical Treatment on Mechanical Properties of Sisal Fiber." *Compos. Interfaces*, 18(6), 527–541.

Kiew Liew, F., Hamdan, S., Rezaur Rahman, M., and Rusop, M. (2017). "Thermomechanical Properties of Jute/Bamboo Cellulose Composite and Its Hybrid Composites: The Effects of Treatment and Fiber Loading." *Adv. Mater. Sci. Eng.*, 2017, 1–10.

Kim, H., Okubo, K., Fujii, T., and Takemura, K. (2013). "Influence of fiber extraction and surface modification on mechanical properties of green composites with bamboo fiber." *J. Adhes. Sci. Technol.*, 27(12), 1–11.

Kiron, M. I. (2011). "Bamboo Fiber|Bamboo Fabric|Production Process of Bamboo Fabric." <http://textilelearner.blogspot.com/2011/12/bamboo-fiber-bamboo-fabric-production.html> (May 24, 2018).

Krishna Adhikari, R., and Keerthi Gowda, B. S. (2017). "Exploration of mechanical properties of banana/jute hybrid polyester composite." *Mater. Today Proc.*, 4(8), 7171–7176.

Krishnan, P. (2015). "Synthesis and Characterization of Cashew Nut Shell Liquid (CNSL) Matrix Compositions for Composites Applications." *Int. Conf. Nat. Polym.*, 1–5.

Kumar, N., and Das, D. (2017). "Fibrous Biocomposites from Nettle (Girardinia diversifolia) and Poly(lactic acid) Fibers for Automotive Dashboard Panel Application." *Compos. Part B Eng.*, 130, 54–63.

Kumar, S., Bhabani, •, Satapathy, K., and Patnaik, A. (2011). "Viscoelastic Interpretations of Erosion Performance of Short Aramid Fibre Reinforced Vinyl Ester Resin Composites." *J. Mater. Sci.*, 46, 7489–7500.

Leandro, A., Silva, D., Renan, L., Silva, R. Da, Andrade Camargo, I. De, Lincon, D., Agostini, D. S., Dos, D., Rosa, S., Lomonaco, D., Oliveira, V. De, Basílio, P., Fechine, A., and Mazzetto, S. E. (2016). "Cardanol-based thermoset plastic reinforced by sponge gourd fibers (Luffa cylindrica)." *Polímeros*, 26(1), 21–29.

Li, Y., Li, Q., and Ma, H. (2015). "The voids formation mechanisms and their effects on

the mechanical properties of flax fiber reinforced epoxy composites." *Compos. Part A Appl. Sci. Manuf.*, 72, 40–48.

Londhe, R., Mache, A., and Kulkarni, A. (2016). "An experimental study on moisture absorption for jute-epoxy composite with coatings exposed to different pH media." *Perspect. Sci.*, 8, 580–582.

Mahmud Zuhudi, N. Z., Jayaraman, K., and Lin, R. J. T. (2016). "Mechanical, Thermal and Instrumented Impact Properties of Bamboo Fabric-Reinforced Polypropylene Composites." *Polym. Polym. Compos.*, 24(9), 79–80.

Mazumdar, S. K. (1977). *Composites Manufacturing Materials, Product and Process Engineering*. CRC Press LLC, 2000 N.W. Corporate Blvd, Florida 33431.

Md Shah, A. U., H Sultan, M. T., Cardona, F., Jawaid, M., Abu Talib, A. R., and Yidris, N. (2017). "Thermal Analysis of Bamboo Fibre and Its Composites." *BioResources*, 12(2), 2394–2406.

Menard, K. P. (1999). *Dynamic Mechanical Analysis - A Practical Introduction*. *J. Pract. Oncol.*, CRC Press LLC, 2000 N.W. Corporate Blvd, Florida 33431.

Meredith, J., Ebsworth, R., Coles, S. R., Wood, B. M., and Kirwan, K. (2012). "Natural fibre composite energy absorption structures." *Compos. Sci. Technol.*, 72(2), 211–217.

Milanese, A. C., Cioffi, M. O. H., and Voorwald, H. J. C. (2012). "Thermal and mechanical behaviour of sisal/phenolic composites." *Compos. Part B Eng.*, 43(7), 2843–2850.

Mittal, V., Saini, R., and Sinha, S. (2016). "Natural Fiber-Mediated Epoxy Composites – A Review." *Compos. Part B Eng.*, 99, 425–435.

Mochane, M. J., Mokhena, T. C., Mokhothu, T. H., Mtibe, A., Sadiku, E. R., Ray, S. S., Ibrahim, I. D., and Daramola, O. O. (2019). "Recent Progress on Natural Fiber Hybrid Composites for Advanced Applications: A Review." *Express Polym. Lett.*, 13(2), 159–198.

Muktha, K., and Keerthi Gowda, B. S. (2017). "Investigation of Water Absorption and Fire Resistance of Untreated Banana Fibre Reinforced Polyester Composites." *Mater. Today Proc.*, 4(8), 8307–8312.

Mustapha, R., Razak, A., and Abdul, R. (2018). "Mechanical and Thermal Properties of Montmorrillonite Nanoclay Reinforced Epoxy Resin with Bio-Based Hardener." *Mater. Today Proc.*, 5(10), 21964–21972.

Nam, T. H., Ogihara, S., and Kobayashi, S. (2012). "Interfacial, Mechanical and Thermal Properties of Coir Fiber-Reinforced Poly(Lactic Acid) Biodegradable Composites." *Adv. Compos. Mater.*, 21(21), 103–122.

Naveen, J., Jawaid, M., Zainudin, E. S., Sultan, M. T. H., Yahaya, R., and Abdul Majid, M. S. (2019). "Thermal Degradation and Viscoelastic Properties of Kevlar/Cocos Nucifera Sheath Reinforced Epoxy Hybrid Composites." *Compos. Struct.*, 219, 194–202.

Nayeem Ahmed, M., and Salman Mustafa, M. (2015). "A Study on Tensile and Compressive Strength of Hybrid Polymer Composite Materials (E Glass Fibre-Carbon Fibre-Graphite Particulate) with Epoxy Resin 5052 by Varying its Thickness." *Int. J. Mech. Eng. Technol.*, 6(4), 17–26.

Ogunsile, B. O., and Oladeji, T. G. (2016). "Utilization of banana stalk fiber as reinforcement in low density polyethylene composite." *Rev. Mater.*, 21(4), 953–963.

Osorio, L., Trujillo, E., Lens, F., Ivens, J., Verpoest, I., and Vuure, A. W. Van. (2018). "In-Depth Study of The Microstructure of Bamboo Fibres and Their Relation to The Mechanical Properties." *J. Reinf. Plast. Compos.*, 37(17), 1–15.

Panda, R., Tjong, J., Nayak, S. K., and Sain, M. M. (2015). "Effect of Alkyl Phenol from Cashew Nutshell Liquid on Mechanical and Dry Sliding Wear Behavior of Epoxy Resin." *BioResources*, 10(3), 4126–4136.

Panwar, V., and Pal, K. (2017). "An Optimal Reduction Technique for rGO/ABS Composites having High-End Dynamic Properties Based on Cole-Cole Plot, Degree of

Entanglement and C-factor." *Compos. Part B Eng.*, 114, 46–57.

Park, S., Baker, J. O., Himmel, M. E., Parilla, P. A., and Johnson, D. K. (2010). "Cellulose Crystallinity Index: Measurement Techniques and Their Impact on Interpreting Cellulase Performance." *Biotechnol. Biofuels*, 3, 1–10.

Pathak, S. K., and Rao, B. S. (2006). "Structural Effect of Phenalkamines on Adhesive Viscoelastic and Thermal Properties of Epoxy Networks." *J. Appl. Polym. Sci.*, 102, 4741–4748.

Porras, A., and Maranon, A. (2012). "Development and Characterization of a Laminate Composite Material From Polylactic Acid (PLA) and Woven Bamboo Fabric." *Compos. Part B Eng.*, 43(7), 2782–2788.

Rahman, M. A., Jasani, A. A., and Ibrahim, M. A. (2017). "Flexural Strength of Banana Fibre Reinforced Epoxy Composites Produced through Vacuum Infusion and Hand Lay-Up Techniques – A Comparative Study." *Int. J. Eng. Mater. Manuf.*, 2(2), 31–36.

Rajesh, M., Singh, S. P., and Pitchaimani, J. (2018). "Mechanical Behavior of Woven Natural Fiber Fabric Composites: Effect of Weaving Architecture, Intra-ply Hybridization and Stacking Sequence of Fabrics." *J. Ind. Text.*, 47(5), 938–959.

Rassiah, K., Hamdan, M. M., Ahmad, M., Ali, A., and Abdullah, A. H. (2017). "Mechanical Properties of Layered Laminated Woven Bamboo Gigantochloa Scortechinii/Epoxy Composites." *J. Polym. Environ.*, 26(4), 1328–1342.

Ratna Prasad, A. V., and Mohana Rao, K. (2011). "Mechanical properties of natural fibre reinforced polyester composites: Jowar, sisal and bamboo." *Mater. Des.*, 32(8–9), 4658–4663.

Rawi, N. F. M., Jayaraman, K., and Bhattacharyya, D. (2013). "A performance study on composites made from bamboo fabric and poly(lactic acid)." *J. Reinf. Plast. Compos.*, 32(20), 1513–1525.

Ridzuan, M. J. M., Majid, M. S. A., Afendi, M., Mazlee, M. N., and Gibson, A. G.

(2016). "Thermal Behaviour and Dynamic Mechanical Analysis of Pennisetum Purpureum/Glass-Reinforced Epoxy Hybrid Composites." *Compos. Struct.*, 152, 850–859.

Rouf, K., Denton, N. L., and French, R. M. (2017). "Effect of Fabric Weaves on The Dynamic Response of Two-Dimensional Woven Fabric Composites." *J. Mater. Sci.*, 52(17), 10581–10591.

Safwan, A., Jawaid, M., Sultan, M. T. H., and Hassan, A. (2018). "Preliminary Study on Tensile and Impact Properties of Kenaf/Bamboo Fiber Reinforced Epoxy Composites." *J. Renew. Mater.*, 6(5), 529–535.

Sahoo, S. K., Mohanty, S., and Nayak, S. K. (2016). "Mechanical, Thermal, and Interfacial Characterization of Randomly Oriented Short Sisal Fibers Reinforced Epoxy Composite Modified with Epoxidized Soybean Oil." *J. Nat. Fibers*, 14(3), 357–367.

Salim, M. S., Rasyid, A., Abdullah, M. A., Taib, R. M., and Mohd Ishak, Z. A. (2018). "Mechanical, Thermal and Flammability Properties of Nonwoven Kenaf Reinforced Acrylic Based Polyester Composites: Effect of Water Glass Treatment." *IOP Conf. Ser. Mater. Sci. Eng. Pap.*, 1–12.

Santos, J. C. dos, Siqueira, R. L., Vieira, L. M. G., Freire, R. T. S., Mano, V., and Panzera, T. H. (2018). "Effects of Sodium Carbonate on The Performance of Epoxy and Polyester Coir-Reinforced Composites." *Polym. Test.*, 67, 533–544.

Sathish, S., Kumaresan, K., Prabhu, L., and Vigneshkumar, N. (2017). "Experimental Investigation on Volume Fraction of Mechanical and Physical Properties of Flax and Bamboo Fibers Reinforced Hybrid Epoxy Composites." *Polym. Polym. Compos.*, 25(3), 229–236.

Segal, L., Creely, J. J., Martin, A. E., and Conrad, C. M. (1959). "An Empirical Method for Estimating the Degree of Crystallinity of Native Cellulose Using the X-Ray Diffractometer." *Text. Res. J.*, 29(10), 786–794.

Shah, A. U. M., Sultan, M. T. H., Jawaid, M., Cardona, F., and Talib, A. R. A. (2016). "A Review on the Tensile Properties of Bamboo Fiber Reinforced Polymer Composites." *BioResources*, 11(4), 10654–10676.

Simon, J. (2005). *Hot Topics in Thermal Analysis and Calorimetry. Therm. Prop. Green Polym.*, (M. E. Brown, ed.), United States of America Visit: Kluwer Academic Publishers.

Singh, V., Kumar, P., and Srivastava, V. K. (2018). "Influence of Cement Particles on the Mechanical and Buckling Behavior of Laminated GFRP Composites with Variation of End Conditions of Buckling." *Mater. Res. Express*, 5(6), 1–11.

Song, Y. S., Lee, J. T., Ji, D. S., Kim, M. W., Lee, S. H., and Youn, J. R. (2012). "Viscoelastic and Thermal Behavior of Woven Hemp Fiber Reinforced Poly(Lactic Acid) Composites." *Compos. Part B Eng.*, 43(3), 856–860.

Sreenivasan, V. S., Rajini, N., Alavudeen, A., and Arumugaprabu, V. (2015). "Dynamic Mechanical and Thermo-Gravimetric Analysis of Sansevieria Cylindrica/Polyester Composite: Effect of Fiber Length, Fiber Loading and Chemical Treatment." *Compos. Part B Eng.*, 69, 76–86.

Srividya, K., Nagaswapnasri, M., Kavitha, E., Anusha, P., and Gopalakrishnaiah, P. (2017). "Experimental and analytical validation of banana and americana hybrid composite." *Int. J. Mech. Eng. Technol.*, 8(6), 384–392.

Sullins, T., Pillay, S., Komus, A., and Ning, H. (2017). "Hemp Fiber Reinforced Polypropylene Composites: The Effects of Material Treatments." *Compos. Part B Eng.*, 114, 15–22.

Suryawanshi, R. T., Venkatachalam, G., and Vimalanand, S. V. (2016). "Determination of Stress Intensity Factor of Banana Fibre Reinforced Hybrid Polymer Matrix Composite Using Finite Element Method." *Period. Polytech. Mech. Eng.*, 60(3), 180–184.

Swamy, M. C., Patil, P., and Chame, S. D. (2016). "Effect of Thickness and Fiber

Orientation on Flexural Strength of GFRP Composites." *Int. J. Adv. Eng. Technol. Manag. Appl. Sci.*, 3(1), 83–93.

Talreja, R., and Varna, J. (2016). *Modeling Damage, Fatigue and Failure of Composite Materials. Woodhead Publ.*

Tong, L., Mouritz, A.P. and Bannister, M. K. (2002). *3D Fibre Reinforced Polymer Composites*.

Tran, L. Q. N., Fuentes, C. A., Dupont-Gillain, C., Vuure, A. W. Van, and Verpoest, I. (2013). "Understanding the interfacial compatibility and adhesion of natural coir fibre thermoplastic composites." *Compos. Sci. Technol.*, 80, 23–30.

Väisänen, T., Das, O., and Tomppo, L. (2017). "A Review on New Bio-Based Constituents for Natural Fiber-Polymer Composites." *J. Clean. Prod.*, 149, 582–596.

Wanderson Moreira Ribeiro, F., Lloyd Ryan Viana Kotzebue, B., Ribeiro Oliveira, J., Francisco Jonas Nogueira Maia, B., Selma Elaine Mazzetto, B., and Lomonaco, D. (2017). "Thermal and Mechanical Analyses of Biocomposites from Cardanol-Based Polybenzoxazine and Bamboo Fibers." *J. Therm. Anal. Calorim.*, 129(1), 281–289.

Wang, C., and Ying, S. (2014). "A Novel Strategy for the Preparation of Bamboo Fiber Reinforced Polypropylene Composites." *Fibers Polym.*, 15(1), 117–125.

Wang, F., Lu, M., Zhou, S., Lu, Z., and Ran, S. (2019). "Effect of Fiber Surface Modification on The Interfacial Adhesion and Thermo-Mechanical Performance of Unidirectional Epoxy-Based Composites Reinforced with Bamboo Fibers." *Molecules*, 24(15).

Wypych, G. (2016). *Handbook of fillers*. ChemTec.

Xu, Z., Yang, F., Guan, Z. W., and Cantwell, W. J. (2016). "An Experimental and Numerical Study on Scaling Effects in the Low Velocity Impact Response of CFRP Laminates." *Compos. Struct.*, 154, 69–78.

Yan, L., Chouw, N., and Yuan, X. (2012). "Improving the mechanical properties of

natural fibre fabric reinforced epoxy composites by alkali treatment." *J. Reinf. Plast. Compos.*, 31(6), 425–437.

Ying, S., Wang, C., and Lin, Q. (2013). "Effects of Heat Treatment on the Properties of Bamboo Fiber/Polypropylene Composites." *Fibers Polym.*, 14(11), 1894–1898.

Zakikhani, P., Zahari, R., Sultan, M. T. H., and Majid, D. L. (2014). "Extraction and preparation of bamboo fibre-reinforced composites." *Mater. Des.*, 63, 820–828.

Zhang, J., and Xu, S. (2019). "Effect of Chain Length of Cardanol-Based Phenalkamines on Mechanical Properties of Air-Dried and Heat-Cured Epoxies." *Mater. Express*, 9(4), 337–343.

Zhang, K., Wang, F., Liang, W., Wang, Z., Duan, Z., and Yang, B. (2018). "Thermal and Mechanical Properties of Bamboo Fiber Reinforced Epoxy Composites." *Polymers (Basel).*, 10(6), 1–18.

Zuhudi, N. Z. M., Lin, R. J. T., and Jayaraman, K. (2016). "Flammability, Thermal and Dynamic Mechanical Properties of Bamboo-Glass Hybrid Composites." *J. Thermoplast. Compos. Mater.*, 29(9), 1210–1228.

List of Publications

- **Kanaginahal, G. M**., Suresh Hebbar, H., and Kulkarni, S. M. (2019). "Influence of Weave Pattern and Composite Thickness on Mechanical Properties of Bamboo/Epoxy composites." *Mater. Res. Express*, 6(12), 1–13.

- **Kanaginahal, G. M**., Suresh Hebbar, H (2022). " Influence of Weave Pattern and Composite Thickness on Dynamic Mechanical Analysis and Water Absorption Properties of Bamboo/Epoxy Composites." *Iranian Polymer Journal*, Status: Under Review.

Curriculum Vitae

Name	:	Gangadhar M Kanaginahal
Date of Birth	:	14/08/1988
Permanent Address	:	S/O M.B.Kanaginahal, Sai residency, Shiv basav, Barakotri link road, Jayanagar, Dharwad, Karnataka – 580001

Educational qualification :

Degree: **Bachelor of Engineering** [2006-2010]
Specialization: Industrial and Production Engineering
Institute: National Institute of Engineering, Mysore

Degree: **Masters of Technology** [2014-2016]
Specialization: Manufacturing Science and Engineering
Institute: B.M.S. College of Engineering, Bengaluru

Degree: **Doctor of Philosophy**
Specialization: Mechanical Engineering
Institute: National Institute of Technology Karnataka
Registration date: 06/07/2017
Thesis submission date: 23/06/2021